# Zinc oxide (ZnO) based quantum dots for bioimaging applications of lipid nanocarriers

Eloísa Berbel Manaia

NNT: 2016SACLS127

# THÈSE DE DOCTORAT

DE

UNIVERSIDADE ESTADUAL PAULISTA "JÚLIO DE MESQUITA FILHO",
FACULDADE DE CIÊNCIAS FARMACÊUTICAS

ET DE

L'UNIVERSITE PARIS-SACLAY,L'UNIVERSITEPARIS SUD

Programa de Pós-graduação em Ciências Farmacêuticas
ÉCOLE DOCTORALE N°569-Innovation Thérapeutique, du fondamental à l'appliqué

Doutorado em Ciências Farmacêuticas
Spécialité de doctorat : Pharmacotechnie et biopharmacie

Par

**Mlle Eloísa Berbel Manaia**

## Zinc oxide (ZnO) based quantum dots for bioimaging applications of lipid nanocarriers

## Conception de Quantum dots à base d'oxyde de zinc (ZnO) pour des applications en bio-imagerie de nanosystèmes lipidiques

## Pontos Quânticos à base de óxido de zinco (ZnO)para aplicações em bioimagem de nanocarreadores lipídicos

**Thèse présentée et soutenue à Araraquara, le 25may 2016:**
**Directeurs de thèse:**
Mme Claudie Bourgaux, Chargée de recherche,Université Paris-Sud, Directeur de thèse
Mme Leila Aparecida Chiavacci Favorin, Professeur, UNESP-FCFAR, Directeur de thèse
Mme Renata C. K. Kaminski, Professeur, UFS, Co-Directeur de thèse
**Composition du Jury:**
M.Celso V. Santilli, Professeur, UNESP-IQ, Examinateur
Mme. Amélie Bochot, Professeure, Université Paris-Sud, Président du Jury
M. Damien Boyer, Maître de Conférences, SIGMA Clermont, Rapporteur
Mme. Márcia Carvalhode Abreu Fantini, Professeure, USP-IF, Rapporteur

Araraquara – SP
2016

# THÈSE DE DOCTORAT

DE

UNIVERSIDADE ESTADUAL PAULISTA "JÚLIO DE MESQUITA FILHO",
FACULDADE DE CIÊNCIAS FARMACÊUTICAS

ET DE

L'UNIVERSITE PARIS-SACLAY,L'UNIVERSITEPARIS SUD

Programa de Pós-graduação em Ciências Farmacêuticas
ÉCOLE DOCTORALE N°569 - Innovation Thérapeutique, du fondamental à l'appliqué

Doutorado em Ciências Farmacêuticas
Spécialité de doctorat : Pharmacotechnie et biopharmacie

Par

**Mlle Eloísa Berbel Manaia**

## Zinc oxide (ZnO) based quantum dots for bioimaging applications of lipid nanocarriers

## Conception de Quantum dots à base d'oxyde de zinc (ZnO) pour des applications en bio-imagerie de nanosystèmes lipidiques

## Pontos Quânticos à base de óxido de zinco (ZnO)para aplicações em bioimagem de nanocarreadores lipídicos

**Directeurs de thèse:**
Mme Claudie Bourgaux, Chargée de recherche,Université Paris-Sud, Directeur de thèse
Mme Leila Aparecida Chiavacci Favorin, Professeur, UNESP-FCFAR, Directeur de thèse
Mme Renata C. K. Kaminski, Professeur, UFS, Co-Directeur de thèse

Tese apresentada ao programa de Pós Graduação em Ciências Farmacêuticas, Área de Pesquisa e Desenvolvimento de Fármacos e Medicamentos, da Faculdade de Ciências Farmacêuticas, Universidade Estadual Paulista Júlio de Mesquita Filho, como parte dos requisitos para obtenção do título de Doutora em Ciências Farmacêuticas.

Araraquara – SP
2016

**Ficha Catalográfica**
Elaborada Pelo Serviço Técnico de Biblioteca e Documentação
Faculdade de Ciências Farmacêuticas
UNESP – Campus de Araraquara

**M266p** Manaia, Eloísa Berbel
Pontos Quânticos à base de óxido de zinco (ZnO) para aplicações em bioimagem de nanocarreadores lipídicos / Eloísa Berbel Manaia. – Araraquara, 2016
175 f.

Tese (Doutorado) – Universidade Estadual Paulista. "Júlio de Mesquita Filho". Faculdade de Ciências Farmacêuticas. Programa de Pós Graduação em Ciências Farmacêuticas

Orientador: Leila Aparecida Chiavacci Favorin
Orientador no exterior: Claudie Bourgaux
Coorientador: Renata Cristina Kiatkoski Kaminski

1. ZnO. 2. Pontos quânticos. 3. Bioimagem. 4. Nanocarreadores lipídicos. I. Favorin, Leila Aparecida Chiavacci, orient. II. Bourgaux, Claudie, orient. III. Kaminski, Renata Cristina Kiatkoski, coorient. IV. Título.

**CAPES: 40300005**

**ELOÍSA BERBEL MANAIA**

PONTOS QUÂNTICOS À BASE DE ÓXIDO DE ZINCO (ZnO) PARA APLICAÇÕES EM BIOIMAGEM DE NANOCARREADORES LIPÍDICOS

Tese de Doutorado apresentada à Faculdade de Ciências Farmacêuticas da Universidade Estadual Paulista – UNESP, Campus de Araraquara como requisito para a obtenção do título de Doutor em Ciências Farmacêuticas

Araraquara, 25 de maio de 2016.

BANCA EXAMINADORA

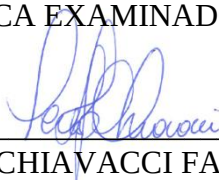

LEILA APARECIDA CHIAVACCI FAVORIN (Orientadora)

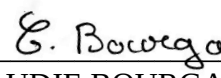

CLAUDIE BOURGAUX

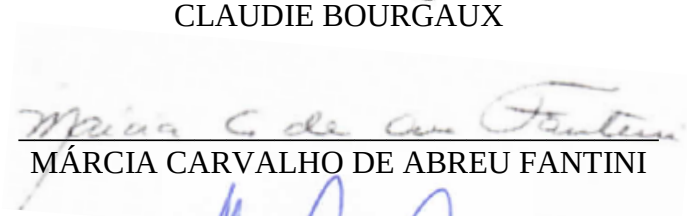

MÁRCIA CARVALHO DE ABREU FANTINI

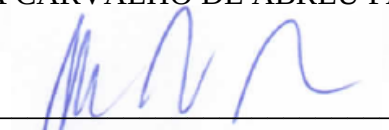

CELSO VALENTIM SANTILLI

DAMIEN BOYER

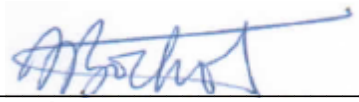

AMÉLIE BOCHOT

**Title :** Zinc oxide (ZnO) based quantum dots for bioimaging applications of lipid nanocarriers

**Keywords :** ZnO, Quantum Dots, bioimaing, and lipid nanocarriers

**Abstract:**Theranostic systems consist of a single device containing therapeutics and diagnosis agents and have increased attention in the actual researches because these devices can improve the disease therapy such as cancer, decrease the side effects and the toxicity in no-cancer cells and permit monitoring the treatment. The aim of this work was to develop theranostic systems consisted of lipid based nanocarriers containing ZnO based quantum dots (QDs) as cancer cell luminescent guides, and a model drug for cancer therapy. Firstly, it was study the synthesis of ZnO/ZnS QDs aiming to achieve improved luminescent properties. In this step, X-Rays Absorption Spectroscopy, together with other usual characterization techniques, could identify the synthesis condition in which core-shell structures were formed. Nevertheless, the emission of ZnO/ZnS QDs in the visible range was not promising. Therefore, Mg-doped ZnO QDs were synthesized and their luminescence went through a maximum for a 20 mol% nominal concentration of $Mg^{2+}$ ions in the reaction medium. $Zn_{0.8}Mg_{0.2}O$ QDs presented quantum yield (QY) six times higher (QY = 64%) than undoped ones (QY = 10%). ZnO and $Zn_{0.8}Mg_{0.2}O$ QDs capped by oleic acid (OA) were synthesized and formed stable colloidal dispersions in chloroform and toluene. The QY of OA-$Zn_{0.8}Mg_{0.2}O$ was about 4 times (around 40%) higher than that of the OA-ZnO QDs. $Zn_{0.8}Mg_{0.2}O$ QDs and OA-$Zn_{0.8}Mg_{0.2}O$ QDs could be incorporated into lipid based nanocarriers of average hydrodynamic diameter around 100 – 220 nm. The luminescent solid lipid nanoparticles (SLN) were stable in different media at 37°C during 3 hours. The fluorescence association study showed enhanced emission of the J774 macrophage-like cells treated with 2 mg/mL of luminescent SLN during 50 min, suggesting partial internalization of the nanoparticles into the macrophages. The internalization study using the video-microscope and fluorescence microscope were not successfully, once the equipment condition used could not overcome the cells auto-fluorescence phenomena.

**Titre :** Conception de Quantum dots à base d'oxyde de zinc (ZnO) pour des applications en bio-imagerie de nanosystèmes lipidiques

**Mots clés :** ZnO, Quantum Dots, bioimagerie etnanosystèmes lipidiques

**Résumé :**Les systèmes théranostiques sont constitués d'un dispositif unique contenant des agents thérapeutiques et diagnostiques et attirent actuellement l'attention pour améliorer le traitement de maladies telles que le cancer ; ils pourraient réduire les effets secondaires (e.g. la toxicité pour les cellules non-cancéreuses) et permettre le suivi du traitement. Les quantum dots (QDs) sont utilisés comme agents d'imagerie *in vitro* et *in vivo*. Parmi ceux-ci, ZnO est moins cher, plus biocompatible et moins toxique que ceux utilisés couramment (SeCd, PbS, etc.). Le but de notre étude était de développer des systèmes théranostiques constitués de nanoparticules lipidiques contenant des QDs à base de ZnO comme agent luminescent, l'objectif final étant d'incorporer un principe actif pour le traitement du cancer. Nous avons d'abord étudié la synthèse de QDs de ZnO/ZnS (structure coeur/coquille) par le procédé sol-gel, afin d'améliorer les propriétés de luminescence de ZnO grâce à la passivation de la surface par le ZnS. Pour cela, deux voies de synthèse ont été explorées: le thioacétamide (TAA), utilisé comme source d'ions soufre, a été ajouté à (i) la solution de précurseur de l'acétate de zinc, et (ii) la suspension colloïdale de ZnO. Différentes concentrations de thioacétamide (TAA) ont été utilisées (1,5, 5 et 50 mM). Pour distinguer la formation de la structure coeur/coquille (ZnO / ZnS) d'un simple melange de particules de ZnO et ZnS, les échantillons ont été caractérisés par plusieurs techniques (DRX, XAS, SAXS, UV-vis, pH, HRTEM et PL). Parmi celles-ci, l'absorption des rayons X (XAS) a été essentielle pour montrer que seule la réaction effectuée à partir de la suspension colloïdale de ZnO contenant 5 mm de TAA donnait lieu à la structure ZnO/ZnS. Cependant, les QDs de ZnO/ZnS n'ont pas montré une intensité de l'émission dans le visible plus grande que celle des QDs de ZnO. Les QDs de ZnO ont donc été dopés pour générer des électrons ou des trous supplémentaires dans leur structure, entraînant des changements de leurs propriétés de luminescence. Différentes quantités de Mg (2,5, 5, 10 et 20% en mole) ont été ajoutées lors de la synthèse du ZnO par la voie sol-gel, afin d'obtenir des particules ayant une luminescenceplus forte dans le visible. Plusieurs techniques (XRD, HRTEM, ICP-MS, SAXS, UV-Vis et PL) ont été utilisées pour déterminer les caractéristiques physico-chimiques des différents $Zn_{1-x}Mg_xO$ QDs obtenus. Il a été observé une diminution de la taille des particules avec l'augmentation de la concentration de Mg. Lors de l'ajout d'une concentration nominale de $Mg^{2+}$ dans le milieu réactionnel de 20% molaire ($Zn_{0.8}Mg_{0.2}O$), le rendement quantique (QY) était six fois plus élevé (QY= 64%) que celui de la suspension de ZnO non dopé (QY= 10%). Pour utiliser les QDs dans un environnement biologique tout en conservant leurs propriétés de photoluminescence, leur surface est généralement modifiée par des substances hydrophiles pour les rendre stables dans l'eau, ou des substances hydrophobes pour permettre leur intégration dans des systèmes/nanoparticules à base de lipides ou de polymères. La surface des QDs de ZnO et $Zn_{0.8}Mg_{0.2}O$ a été recouverte par de l'acide oléique (AO) ; les QDs ainsi modifiés forment une dispersion colloïdale stable dans le chloroforme et le toluène. La spectroscopie Raman a confirmé la présence d'acide oleique à la surface des QDs. Le rendement quantique des QDs de $Zn_{0.8}Mg_{0.2}O$ recouverts d'AO était environ 4 fois plus élevé (QR = 40%) que celui des QDs de ZnO recouverts d'AO. Enfin, les QDs de $Zn_{0.8}Mg_{0.2}O$, recouverts ou non d'AO, ont été incorporés dans des nanoparticules lipidiques pour une utilisation ultérieure dans des études d'internalisation cellulaire. Des formulation à base de DPPC, DSPE-Peg et des nanoparticules lipidiques solides (SLN) contenant des QDs ont été préparées avec une taille hydrodynamique variant entre 100 et 220 nm. Les formulations à base de DSPE-Peg ont montré une intensité d'émission plus élevée dans le visible, comparé aux SLNs. L'étude de stabilité réalisée avec des SLNs luminescentes dans différents milieux (eau, PBS, PBS avec du Mg et du Ca, RPMI avec du sérum à 10%) à 37°C pendant 3 heures a montré que la taille ne changeait pas

fortement au cours du temps. Dans cette étude, la taille maximale était de l'ordre de 300 nm, montrant que même en présence de protéines, il ne se forme pas de gros agrégats. Trois méthodes ont été utilisées pour l'étude de l'internalisation cellulaire dans des macrophages J774. Lorsque la longueur d'onde d'excitation correspond à celle des QDs, les mesures d'intensité de fluorescence sur les suspensions de cellules ont montré une faible augmentation de l'intensité de l'émission visible pour les cellules incubées avec 2 mg/mL de SLNs luminescentes pendant 50 minutes, en comparaison avec les cellules témoins. Ce résultat suggère une internalisation partielle des SLNs dans les macrophages. Malheureusement, ces résultats n'ont pas pu être confirmés par vidéo-microscopie et microscopie de fluorescence sur les cellules parce que les conditions expérimentales ( longueurs d'onde d'excitation et d'émission possibles) ne permettaient pas d'observer un signal supérieur à celui de l'auto-fluorescence des cellules.

En conclusion, cette étude a permis d'optimiser la composition et la synthèse par voie sol-gel de QDs à base de ZnO pour les rendre aptes à être utilisés comme sondes luminescentes dans des nanoparticules lipidiques. La relation entre leur structure et leurs propriétés de luminescence a été étudiée; les QDs dopés $Zn_{0.8}Mg_{0.2}O$, qui ont le rendement quantique le plus élevé, ont pu être incorporés dans des nanoparticules lipidiques pouvant contenir des agents thérapeutiques.

**Título :**Pontos Quânticos à base de óxido de zinco (ZnO) para aplicações em bioimagem de nanocarreadores lipídicos

**Palavras-chaves :** ZnO, Pontos Quânticos, bioimageme nanocarreadores lipídicos

**Resumo :**Sistemas teranósticos consistem em um único dispositivo contendo agentes terapêuticos e de diagnóstico e tem ganhado atenção nas pesquisas atuais por melhorar o tratamento de doenças como câncer, podendo diminuir efeitos colaterais, diminuir toxicidade em células não cancerígenas e permitir o monitoramento do tratamento. Os pontos quânticos (PQs) vem sendo usado como agentes de imagem para realizar o monitoramento ótico em investigações *in vivo* e *in vitro*. Dentre eles, o ZnO tem se destacado por ser mais barato, mais biocompatível e menos tóxico do que os utilizados comumente (SeCd, PbS, etc). O objetivo deste trabalho foi desenvolver sistemas teranósticos constituídos de nanocarreadores à base de lipídeos contendo pontos quânticos a base de ZnO, como guias luminescentes de células cancerígenas, e um fármaco modelo para tratamento do câncer. Primeiramente, foi estudada a síntese de pontos quânticos de ZnO/ZnS (estrutura de casca/caroço) pelo processo sol-gel, a fim de melhorar as propriedades luminescentes do ZnO através da passivação da sua superfície provocada pelo ZnS. Para isto, as reações de síntese tiveram como base (i) a solução precursora de acetato de Zinco e (ii) a suspensão coloidal de ZnO. Além disso, foram variadas as concentrações de tioacetamida (TAA) (1.5, 5 e 50mM), usada como fonte de íons de enxofre. Para diferenciar a formação de estruturas casca/caroço (ZnO/ZnS) e não uma mistura de partículas de ZnO e ZnS, várias técnicas foram utilizadas para caracterizar as amostras (DRX, XAS, SAXS, UV-vis, pH, HRTEM e PL). Dentre elas, XAS foi crucial para identificar que somente a reação realizada a partir da suspensão coloidal de ZnO com TAA 5mM deu origem à estrutura de ZnO/ZnS do tipo casca/caroço. Entretanto, os PQs de ZnO/ZnS não apresentaram maior intensidade da emissão na região do visível quando comparado ao ZnO. Portanto, PQs de ZnO foram dopados com Mg para gerar elétrons ou buracos extras na sua estrutura levando a mudanças em suas propriedades luminescentes. Diferentes quantidades de Mg (2.5, 5, 10 e 20 % em mol) foram usadas durante a síntese de ZnO pelo processo sol-gel para poder obter, assim, partículas com maior luminescência na região do visível. DRX, HRTEM, ICP-MS, SAXS, UV-Vis e PL foram usadas a fim de avaliar as características físico-químicas dos diferentes $Zn_{1-x}Mg_xO$ obtidos. Observou-se a diminuição do tamanho das partículas com o aumento da concentração de Mg. Quando se utilizou 20 % em mols em concentração nominal de íons $Mg^{2+}$ no meio reacional ($Zn_{0.8}Mg_{0.2}O$), o rendimento quântico (RQ) foi seis vezes maior (RQ = 64%) do que a suspensão de ZnO não dopado (RQ = 10%). Para utilizar os PQs em meio biológico mantendo sua propriedade fotoluminescente, sua superfície normalmente é modificada com substâncias hidrofílicas para torná-los estáveis em água, ou com substâncias hidrofóbicas para permitir sua incorporação em sistemas/carreadores à base de lipídeos ou polímeros. Os PQs de ZnO e de $Zn_{0.8}Mg_{0.2}O$ foram revestidos com ácido oleico (AO) formando uma dispersão coloidal estável em clorofórmio e tolueno. A espectroscopia RAMAN permitiu confirmar a modificação da superfície dos PQs pela presença dos grupamentos característicos do AO nessas amostras. O RQ do $Zn_{0.8}Mg_{0.2}O$ revestido com AO foi em torno de 4 vezes maior (RQ = 40%) que o RQ de ZnO revestido com AO. Por fim, os PQs de $Zn_{0.8}Mg_{0.2}O$ revestidos e não-revestidos com AO foram incorporados em nanocarreadores lipídicos para serem utilizados posteriormente nos estudos de internalização celular. Formulações à base de DPPC, DSPE-Peg e nanopartículas lipídicas sólidas (NLS) contendo PQs foram obtidos com diâmetro hidrodinâmico entre 100-220 nm. A formulação preparada com DSPE-Peg apresentou maior intensidade de emissão no visível quando comparadas com as NLS. O estudo de estabilidade realizado com as NLS luminescentes em diferentes meios (água, PBS, PBS com Mg e Ca, RPMI com soro à 10%) à 37°C durante 3 horas, mostrou que o tamanho delas não variou bruscamente no tempo analisado. Nesse estudo o tamanho máximo

encontrado foi de 300 nm, mostrando que na presença de proteínas, elas não formam grandesagregados que podem favorecer a fagocitose pelo sistema mononuclear. Foram utilizados três métodos para realizar o estudo de internalização celular. O estudo da associação de fluorescência mostrou aumento da intensidade de emissão no visível de células de macrófagos J774 tratadas com 2 mg/mL de NLS luminescente durante 50 min, comparado com as células sem tratamento. Este resultado sugere internalização parcial das NLS nos macrófagos. A vídeo-microscopia e a microscopia de fluorescência não tiveram sucesso para realizar este estudo, uma vez queas condições experimentais utilizadas não puderam superar o efeito de auto-fluorescência das células. Para concluir, a síntese de PQs à base de ZnO pelo processo sol-gel possibilitou estudar as estruturas e propriedades luminescentes destes, permitindo otimizar sua síntese para adequá-los para uso como guias luminescentes. Desta forma, $Zn_{0.8}Mg_{0.2}O$ com alto rendimento quântico foi incorporado em nanocarreadores lipídicos e sua aplicação como guia luminescente foi evidenciada através do teste de associação de fluorescência.

# *Acknowledgements*

Firstly, I thank **God** for always guide me.

**Bruno** by his company, motivation, knowledge, help, good humor, love and affection.

To my family, especially my parents, **Cida** and **Osvaldo**, my sisters **Juliana** and **Mariele**, my brother in law **Eduardo** and my nieces **Sarah**, **Luana** and **Rafaela** by their love and encouragement.

I thank my supervisors Prof. Dr. **Leila Aparecida ChiavacciFavorin** and Dr. **Claudie Bourgaux** and my co-advisor Dr. **Renata C. K. Kaminski** for their dedication, supervision, motivation, and patience.

My friends of **CMAF laboratoryMarina**, **BrunaLallo**, **Bruna Chiari**, **Neima**, **Gabriela**, **João**, **Mariluci**, **Flavia**, **Aline** and **Natalia** for their help, support, and also **Mariana Sato, Jéssica and Alice**.

The friendships of **Institut GaIienAndreza**, **Any**, **André**, **Júnior**, **Thais**, **Benedict**, **Cristina**, **Leila**, **Chau**, **Boris**, **Frank**, **Elodie, Sarah** and also Dr. **François-XavierLegrand**, Dr. **Vincent Faivre**, **Jean-Jacques**, **David**, Dr. **Angélina Angelova**, **Fany**, Dr. **Gillian Barratt**, **Claire**, **Alice**, **Fatima**, Dr. **Christine Vauthier**, Dr. **Didier Desmaele** and Dr. **Sylviane Lesieur**.

The Brazilian friends that I met in France **Sara Bachner**, **Rodrigo** (Dido), **Dani, Kellen** and all those that were visit me when I was in Paris **Má**, **Sarah**, **Cidinha**, **Patty**, **Marina**, **Roberto**, **Milena**, **Tia Rô**, **Carol**, **André** (Presidente), Mrs **Sonia**, Mr **Antônio, Gisele**, **Cavalim**,**Tia Eliana**, **Tia Eloísa**, **Daniel** and those that we met by chance **Marcel,Natália**, **Milana** and **Gledson.**

The Brazilian neighbors of 1, Rue Gustave Geffroy, **Sarah** and **Helena**, lovely women.

The **Chemical Institute** of UNESP/Araraquara, especially teachers Dr. **Celso V. Santilli**, Dr. **Sandra Helena Pulcineli**, Dr. **Peter Hammer**, the colleagues **Nalva**, **Aline**, **Bianca**, **Marlon, Rodrigo, Rodolfo** and specially **Marina** and **Amélie** for their supporting during HRTEM and EXAFS understandings, respectively, and the laboratory technicians **Sérgio, Rafael** and **Ricardo**.

The synchrotron **SOLEIL** for providing beamtime at the SAMBA beamline (project number: 20131299),Dr. **Valérie Briois** for her support during EXAFS experiments and all her knowledge, discussions, and help during my thesis; SWING beamline (project number: 20131299**) J. Perez**, **Y. Liatimi** and **Pierre Roblin** for their support during SAXS experiments; **Stéphanie Blanchandin** and **Karine Chaouchi** for WAXS measurements and their kindly support at the Chemistry Laboratory of SOLEIL.

The **LNLS** (project number: 14321) for SAXS measurements, Dr. **Florian Meneau** for his support during SAXS understanding, motivation and friendship, **LNNano** for HRTEM measurements.

The **Service of electronic microscopy** of the University Pierre et Marie Curie for HRTEM measurements.

The secretaries of **Post-GraduationTechnique Section of Facultyof PharmaceuticalSciences**, **Claudia**, **Daniela**, **Joyce**, **Flávia** and the secretary of **Doctoral School"Innovation thérapeutique du fondamental à l'appliqué"** Mme **Lucie Landry**.

**FAPESP**(Process number: 2012/07570-4 and BEPE process number: 2015/01198-4) and **PADC/FCF-UNESP** for the financial support.

My thesis was conducted at the Institut Galien of University Paris - Sud during one year supported by the International Cooperation Program **CAPES/COFECUB** (ME 767-13), financed by CAPES – Brazilian Federal Agency for Support and Evaluation of Graduate Education within the Ministry of Education of Brazil.

To all those who directly or indirectly contributed to the realization of this thesis, thank you very much.

# List of Figures

# List of tables

# List of abbreviations

Ab: antibody

AET: aminoethanethiol-HCl

AFM : atomic force microscopy

CMC: critical micellar concentration

Cryo-TEM: cryogenic transmission electron microscopy

CT :Computed Tomography

DPPC: 1,2-dipalmitoyl-sn-glycero-3-phosphocholine

DSPE-Peg:1,2-distearoyl-sn-glycero-3-phosphoethanolamine-N-[amino(polyethylene glycol)-2000] ammonium salt

EGFR: epidermal growth factor receptor

EPR: enhanced permeation and retention

EXAFS: extended X-ray absorption fine structure

FT: Fourier transform

FWHM: full width at half maximum

GUV: giant unilamellar vesicles

HA: hyaluronic acid

HepG2: human liver carcinoma cells

HDS: hydroxy double salts

HRTEM: High Resolution Transmission Electron Microsocpy

ICP – MS: Inductively Coupled Plasma Mass Spectrometry

J774: murine phagocytic macrophage-like cell line

LCF: Linear Combination Fittings

LNC: lipid nanocapsules

LUV: large unilamellar vesicles

MHDA: 16-mercaptohexadecanoic acid

MLV: multilamellar vesicles

MOF: metal organic frameworks

MPS: mononuclear phagocyte system

MRI: magnetic resonance imaging

MUA: 11-mercaptoundecanoic acid

NCs: nanocarriers

NIR: near-infrared

NPs: Nanoparticles

OA: oleic acid

OA-ZnO QDs: ZnO quantum dots with oleic acid as surface modifier

OA- $Zn_{1-x}Mg_xO$ QDs: Mg-doped ZnO quantum dots with oleic acid as surface modifier

PBS:Phosphate-buffered saline

PEG: polyethylene glycol

PL: Photoluminescence

PLE : excitation photoluminescence

PREC: precursor

QDs: quantum dots

QD-LN: SLNs containing $Zn_{0.8}Mg_{0.2}O$ QDs

QELS: Quasi Elastic Ligth Scattering

QY: Quantum Yield

RES: reticuloendothelial system

RF: red phenol

Rg: radius of gyration

ROS: reactive oxygen species

RPMI: Roswell Park Memorial Institute, medium of cell culture

SAXS: Small Angle X-Ray Scattering

SLN: solid lipid nanoparticles

SR: synchrotron radiation

SUSP: Suspension

SUV: Small unilamellar vesicles

TAA: Thioacetamide

THF: tetrahydrofuran

UV-vis: ultravioleta-visible

XANES: X-ray absorption near-edge structure

XAS: X-Ray Absorptions Spectroscopy

XDR: X-Ray Diffraction

XES: X-ray emission spectroscopy

XPS: X-ray Photoelectron Spectroscopy

ZnO Susp: ZnO colloidal suspensions

$Zn_{1-x}Mg_xO$ QDs: Mg-doped ZnO quantum dots with x amount of Mg

# CONTENT

CHAPTER VI – Final conclusions and Perspectives

# INTRODUCTION

# Introduction

The use of nanotechnology in the biomedical field is increasing due to the advantages of drug nanocarriers. For instance, nanoparticles loaded with drugs may improve the solubility and bioavailability of poorly soluble drugs, protect them from degradation, cross biological barriers, decrease drug toxicity against healthy cells by delivering the drug in target tissues. The drug loading capacity, biodistribution, pharmacokinetics and toxicity of nanoparticles depend on their composition, size, structure and surface properties. For example, nanoparticle surface modification by hydrophilic polymers or specific ligands has been explored to promote longer circulation time or to guide them to target tissue. Lipid based nanocarriers, such as liposomes, phospholid micelles and solid lipid nanoparticles,are widely imvestigated due to their biocompatibility and biodegradability.

Theranostic devices arise from the combination of therapeutic and imaging agents in a unique nanoparticle, in order to follow the nanoparticle biodistribution and to evaluate the disease evolution.

Numerous imaging agents can be used in theranostic nanoparticles, depending on the type of image: radionuclides for nuclear imaging, heavy elements for computed tomography,superparamagnetic metal oxides for magnetic resonance imaging and fluorescent dyes or quantum dots (QDs) for optical imaging. QDs have gained place because they present original properties, such as alarge absorption spectrum, a narrow emission band and bright signal. Cadmiun (Cd) based QDs were the first and most explored QDs for bioimaging application; however, they present high toxicity as well as other heavy metal based QDs. To minimize the toxic effects, core-shell QDs and surface capped QDs were developed in order to prevent the release of heavy ions in the biological media. Moreover, coating QDs with a higher band gap semiconductor can eliminate surface defects, which minimizes the photoblinking effect, and QDs surface modification with organic molecules can provide colloidal stability in aqueous media or non-polar solvents. Nevertheless, nontoxic QDs, such as ZnO or ZnS QDs, began to be used due to their biocompatility and promising photoluminescent properties.

The photoluminescence of ZnO QDs is directly related to their size and surface defects. Because of these important characteristics, the synthesis route strongly interferes with the final properties of the material. Since 1980, researchers have studied the quantum confinement and luminescent properties of ZnO QDs synthesized using the sol-gel route,

which allows obtaining nanoparticles with size varying from 2 to 6 nm, displaying surface defects such as oxygen vacancies. However, the visible luminescence of ZnO QDs vanishes in the presence of water because they tend to aggregate, precipitate and their luminescent centers are destroyed. For this reason, the challenge is to keep their visible photoluminescence emission in biological media to allow their use in bioimaging.

The aim of this work was to develop ZnO based QDs with strong visible emission, stable in biological media or organic solvent that allow their later incorporation in lipid based nanocarriers, in order to achieve theranostic devices.

In the first part (Chapter III), ZnO/ZnS core-shell QDs were developed using a low-temperature sol-gel route. The formation of ZnS shell around the ZnO core could provide UV photoluminescence stability and prevent photoblinking and photobleaching undesirable effects. Numerous techniques, such as Small Angle X-Ray Scattering (SAXS), UV-Vis Spectroscopy, pH, X-Ray Absorption (XAS), High Resolution Transmission Electron Microscopy (HRTEM)), X-Ray Diffraction (XRD) were used to monitor the reactions and characterize the materials obtained. When characterized by Photoluminescence Spectroscopy, ZnO/ZnS core-shell QDs did not present an increase in the emission intensity in the visible range.

Because of ZnO/ZnS structures did not demonstrate desirable optical properties, the optimization of ZnO QDs for imaging was performed differently. Chapter IV described ZnO QDs doped with $Mg^{2+}$ ions with enhanced luminescence emission. Specifically, we have shown that the maximum quantum yield (QY = 64%) for Mg precursor concentration of 20 mol% was six times higher than for undoped ZnO QDs (QY = 10%). Mg-doped ZnO QDs were characterized in order to establish a relationship between the composition and structure of the QDs and their luminescent properties.

The surface modification of the QDs was then performed using oleic acid (OA) to hinder their aggregation and to provide them colloidal stability in non-polar environment. Still in the Chapter IV, we could show that Mg-doped ZnO QDs capped by OA formed stable colloidal suspensions in toluene and chloroform, while preserving their photoluminescence with QY around 40 %, promising for bioimaging.

In the Chapter V, the OA surface modified Mg-doped QDs were incorporated in lipid based nanocarriers in order to analyze the nanoparticles structure, stability and luminescence. At low QD concentrations, QDs were embedded within 1,2-dipalmitoyl-sn-glycero-3-phosphocholine (DPPC) bilayers, without perturbing their stacking. 1,2-distearoyl-sn-glycero-

3-phosphoethanolamine-N-[amino(polyethylene glycol)-2000] ammonium salt(DSPE-Peg) /QDs formulations formed aggregates displaying a close-packed, layered structure, of QDs likely stabilized by a layer of DSPE-Peg. Solid lipid nanoparticles (SLN) loaded with QDs demonstrated good stability in biological media as shownby the absence of large aggregates. Cell internalization studies using luminescent SLN were performed using a macrophage-like cell line. However, cell autofluorescence prevented to unambiguously evidence the internalization of SLN into the cells.

## I.4. REFERENCES

ABDULLAH AL; N. LEE, J.E.; IN, I.; LEE, H.; LEE, K.D.; JEONG, J.H.; PARK; S.Y. Target Delivery and Cell Imaging Using Hyaluronic Acid-Functionalized Graphene Quantum Dots. **Mol Pharm,** v. 10, n. 10, p. 3736-3744, 2013.

ABDULLAH, M.; MORIMOTO, T.; OKUYAMA, K. Generating Blue and Red Luminescence from ZnO/Poly(ethylene glycol) Nanocomposites Prepared Using an In-Situ Method. **Adv Funct Mater,** v. 13, n. 10, p. 800-804, 2003.

ABOULAICH, A., TILMACIU, C.-M., MERLIN, C., MERCIER, C., GUILLOTEAU, H., MEDJAHDI, G., SCHNEIDER, R. Physicochemical properties and cellular toxicity of (poly)aminoalkoxysilanes-functionalized ZnO quantum dots. **Nanotechnology**, v. 23, p. 335101:1-9, 2012.

ACHARYA, S.; SAHOO, S. K. PLGA nanoparticles containing various anticancer agents and tumour delivery by EPR effect. **Adv Drug Deliv Rev,** v. 63, n. 3, p. 170-183, 2011.

ALLEN, T. M.; CULLIS, P. R. Liposomal drug delivery systems: From concept to clinical applications. **Adv Drug Deliv Rev,** v. 65, n. 1, p. 36-48, 2013.

BAHNEMANN, D. W.; KORMANN, C.; HOFFMANN, M. R. Preparation and characterization of quantum size zinc oxide: a detailed spectroscopic study. **J Phys Chem,** v. 91, n. 14, p. 3789-3798, 1987.

BARENHOLZ, Y. Doxil® — The first FDA-approved nano-drug: Lessons learned. **J Control Release,** v. 160, n. 2, p. 117-134, 2012.

BAUM, R. P.; KULKARNI, H. R. THERANOSTICS: From Molecular Imaging Using Ga-68 Labeled Tracers and PET/CT to Personalized Radionuclide Therapy - The Bad Berka Experience. **Theranostics**, v. 2, n. 5, p. 437-447, 2012.

BELOGLAZOVA, N. V.;SHMELIN, P.S.; SPERANSKAYA, E.S.; LUCAS, B.; HELMBRECHT, C.; KNOPP, D.; NIESSNER, R.; DE SAEGER, S.; GORYACHEVA, I.Y. Quantum Dot Loaded Liposomes As Fluorescent Labels for Immunoassay. **Anal Chem,** v. 85, n. 15, p. 7197-7204, 2013.

BHASKAR, S. TIAN, F.; STOEGER, T.; KREYLING, W.; DE LA FUENTE, J. M.; GRAZÚ, V.; BORM, P.; ESTRADA, G.; NTZIACHRISTOS, V.; RAZANSKY, D. Multifunctional Nanocarriers for diagnostics, drug delivery and targeted treatment across blood-brain barrier: perspectives on tracking and neuroimaging. **Part Fibre Toxicol,** v. 7, n. 1, p. 1-25, 2010.

BRIOIS, V. GIORGETTI, C.H.; BAUDELET,F.;BLANCHANDIN, S.; TOKUMOTO, M. S.; PULCINELLI,S. H.; SANTILLI, C. V. Dynamical Study of ZnO Nanocrystal and Zn-HDS Layered Basic Zinc Acetate Formation from Sol−Gel Route. **J Phys Chem CNanomater Interfaces,** v. 111, n. 8, p. 3253-3258, 2007.

BRUNETTI, V. CHIBLI, H.; FIAMMENGO, R.; GALEONE, A.; MALVINDI, M. A.; VECCHIO, G.; CINGOLANI, R.; NADEAU, J. L.; POMPA, P. P.InP/ZnS as a safer alternative to CdSe/ZnS core/shell quantum dots: in vitro and in vivo toxicity assessment. **Nanoscale,** v. 5, n. 1, p. 307-317, 2013.

BRUS, L. E. A simple model for the ionization potential, electron affinity, and aqueous redox potentials of small semiconductor crystallites. **J Chem Phys,** v. 79, n. 11, p. 5566-5571, 1983.

BUONSANTI, R.; MILLIRON, D. J. Chemistry of Doped Colloidal Nanocrystals. **Chem Mater,** v. 25, n. 8, p. 1305-1317, 2013.

CAETANO, B. L. SANTILLI, C. V.; MENEAU, F.; BRIOIS, V.; PULCINELLI, S. H.In Situ and Simultaneous UV−vis/SAXS and UV−vis/XAFS Time-Resolved Monitoring of ZnO Quantum Dots Formation and Growth. **J Phys Chem CNanomater Interfaces,** v. 115, n. 11, p. 4404-4412, 2011.

CAMBLIN, M.;DETAMPEL, P.; KETTIGER, H.; WU, D.; BALASUBRAMANIAN, V.; HUWYLER, J. Polymersomes containing quantum dots for cellular imaging. **Int J Nanomedicine,** v. 9, p. 2287-2298, 2014.

CASSETTE, E.;PONS, T.; BOUET, C.; HELLE, M.; BEZDETNAYA, L.; MARCHAL, F.; DUBERTRET, B. Cu−In−Se/ZnS Core/Shell Quantum Dots for In vivo Imaging. **Chem Mater,** v. 22, n. 22, p. 6117-6124, 2010.

CHEN, O.;ZHAO, J.; CHAUHAN, V. P.; CUI, J.; WONG, C.; HARRIS, D. K.; WEI, H.; HAN, H. S.; FUKUMURA, D.; JAIN, R. K.; BAWENDI, M. G. Compact high-quality CdSe–CdS core–shell nanocrystals with narrow emission linewidths and suppressed blinking. **Nat Mater,** v. 12, n. 5, p. 445-451, 2013.

CHO, S. J.; MAYSINGER, D.; JAIN, M.; RÖDER, B.; HACKBARTH, S.; WINNIK, F. M.Long-Term Exposure to CdTe Quantum Dots Causes Functional Impairments in Live Cells. **Langmuir,** v. 23, n. 4, p. 1974-1980, 2007.

COHN, A. W.; KITTILSTVED, K. R.; GAMELIN, D. R. Tuning the Potentials of “Extra” Electrons in Colloidal n-Type ZnO Nanocrystals via Mg2+ Substitution. **J Am Chem Soc,** v. 134, n. 18, p. 7937-7943, 2012.

CONNIOT, J. SILVA, J. M., FERNANDES, J. G., SILVA, L. C., GASPAR, R., BROCCHINI, S., FLORINDO, H. F., BARATA, T. S. Cancer immunotherapy: nanodelivery approaches for immune cell targeting and tracking. **Front Chem,** v. 2, p. 1-27, 2014.

CONTRERAS, E. Q.; CHO, M.; ZHU, H.; PUPPALA, H. L.; ESCALERA, G.; ZHONG, W.; COLVIN, V.L.Toxicity of Quantum Dots and Cadmium Salt to Caenorhabditis elegans after Multigenerational Exposure. **Environ Sci Technol,** v. 47, n. 2, p. 1148-1154, 2013.

DAOU, T. J.; LI, L.; REISS, P.; JOSSERAND, V.; TEXIER, I. Effect of Poly(ethylene glycol) Length on the in Vivo Behavior of Coated Quantum Dots. **Langmuir,** v. 25, n. 5, p. 3040-3044, 2009.

DAZZAZI, A.; COPPEL, Y.; IN, A.; CHASSENIEUX, C.; MASCALCHI, P.; SALOMÉ, L.; BOUHAOUSS, A.; KAHN, M. L.; GAUFFRE, F. Oligomeric and polymeric surfactants for the transfer of luminescent ZnO nanocrystals to water. **J Mater Chem C,** v. 1, n. 11, p. 2158-2165, 2013.

DE JONG, W. H.; BORM, P. J. A. Drug delivery and nanoparticles: Applications and hazards. **Int J Nanomedicine,** v. 3, n. 2, p. 133-149, 2008.

DERFUS, A. M.; CHAN, W. C. W.; BHATIA, S. N. Probing the Cytotoxicity of Semiconductor Quantum Dots. **Nano Lett,** v. 4, n. 1, p. 11-18, 2004.

DESMAËLE, D.; GREF, R.; COUVREUR, P. Squalenoylation: A generic platform for nanoparticular drug delivery. **J Control Release,** v. 161, n. 2, p. 609-618, 2012.

DONG, Y.;NG, W. K.; SHEN, S.; KIM, S.; TAN, R. B.. Solid lipid nanoparticles: Continuous and potential large-scale nanoprecipitation production in static mixers. **Colloids Surf B Biointerfaces.,** v. 94, n. 0, p. 68-72, 2012.

DUBERTRET, B.; SKOURIDES, P.; NORRIS, D. J.; NOIREAUX, V.; BRIVANLOU, A. H.; LIBCHABER, A.In Vivo Imaging of Quantum Dots Encapsulated in Phospholipid Micelles. **Science,** v. 298, n. 5599, p. 1759-1762, 2002.

EFROS, A.L. Interband absorption of light in a semiconductor sphere. **Sov Phys Semicond**, v.16, p. 772–775, 1982.

FATTAL, E.; TSAPIS, N. Nanomedicine technology: current achievements and new trends. **Clin Transl Imaging,** v. 2, n. 1, p. 77-87, 2014.

FERRO-FLORES, G.;OCAMPO-GARCÍA, B. E.; SANTOS-CUEVAS, C. L.; DE MARÍA RAMÍREZ, F.; AZORÍN-VEJA, E. P.; MELÉNDEZ-ALAFORT, L. Theranostic Radiopharmaceuticals Based on Gold Nanoparticles Labeled with $^{177}$Lu and Conjugated to Peptides. **Curr Radiopharm,** v. 8, n. 2, p. 150-159, 2015.

FORTIN-RIPOCHE, J.-P.;MARTINA, M. S.; GAZEAU, F.; MÉNAGER, C.; WILHELM, C.; BACRI, J. C.; LESIEUR, S.; CLÉMENT, O.Magnetic Targeting of Magnetoliposomes to Solid Tumors with MR Imaging Monitoring in Mice: Feasibility. **Radiology,** v. 239, n. 2, p. 415-424, 2006.

FRANK, D.;TYAGI, C.; TOMAR, L.; CHOONARA, Y. E.; DU TOIT, L. C.; KUMAR, P.; PENNY, C.; PILLAY, V. Overview of the role of nanotechnological innovations in the detection and treatment of solid tumors. **Int J Nanomedicine,** v. 9, p. 589-613, 2014.

FU, Y.-S.; DU, X. W.; KULINICH, S. A.; QIU, J. S.; QIN, W. J.; LI, R.; SUN, J.; LIU, J. Stable Aqueous Dispersion of ZnO Quantum Dots with Strong Blue Emission via Simple Solution Route. **J Am Chem Soc,** v. 129, n. 51, p. 16029-16033, 2007.

GABIZON, A.;CATANE, R.; UZIELY, B.; KAUFMAN, B.; SAFRA, T.; COHEN, R.; MARTIN, F.; HUANG, A.; BARENHOLZ, Y. Prolonged Circulation Time and Enhanced Accumulation in Malignant Exudates of Doxorubicin Encapsulated in Polyethylene-glycol Coated Liposomes. **Cancer Res,** v. 54, n. 4, p. 987-992, 1994.

GAO, X.; CUI. Y.; LEVENSON, R. M.; CHUNG, L. W.; NIE, S. In vivo cancer targeting and imaging with semiconductor quantum dots. **Nat Biotech,** v. 22, n. 8, p. 969-976, 2004.

GILL, R.; ZAYATS, M.; WILLNER, I. Semiconductor Quantum Dots for Bioanalysis. **Angew Chem Int Ed Engl,** v. 47, n. 40, p. 7602-7625, 2008.

GOLDMAN, E. R.;BALIGHIAN, E. D.; MATTOUSSI, H.; KUNO, M. K.; MAURO, J. M.; TRAN, P. T.; ANDERSON, G. P. Avidin: A Natural Bridge for Quantum Dot-Antibody Conjugates. **J Am Chem Soc,** v. 124, n. 22, p. 6378-6382, 2002.

GREGORIADIS, G.; RYMAN, B. E. Liposomes as carriers of enzymes or drugs: a new approach to the treatment of storage diseases. **Biochem J,** v. 124, n. 5, p. 58P, 1971.

HAMMAD, T. M.; SALEM, J. K.; HARRISON. R. G.; HEMPELMANN, R.; HEJAZY. N. K.Optical and magnetic properties of Cu-doped ZnO nanoparticles. **J Mater Sci: Mater Electron,** v. 24, n. 8, p. 2846-2852, 2013.

HAN, H.-S.;NIEMEYER, E.; HUANG, Y.; KAMOUN, W. S.; MARTIN, J. D.; BHAUMIK, J.; CHEN, Y.; ROBERGE, S.; CUI, J.; MARTIN, M. R.; FUKUMURA, D.; JAIN, R. K.; BAWENDI, M. G.; DUDA, D.G. Quantum dot/antibody conjugates for in vivo cytometric imaging in mice. **Proc Natl Acad Sci U S A.,** v. 112, n. 5, p. 1350-1355, 2015.

HAN, L.-L.;CUI, L.; WANG, W.-H.;WANG, J.-L.; DU, X.-W.On the origin of blue emission from ZnO quantum dots synthesized by a sol–gel route. **Semicond Sci Technol,** v. 27, n. 6, p. 8, 2012.

HANN, I. M.; PRENTICE, H. G. Lipid-based amphotericin B: a review of the last 10 years of use. **Int J Antimicrob Agents,** v. 17, n. 3, p. 161-169, 2001.

HARDMAN, R. A Toxicologic Review of Quantum Dots: Toxicity Depends on Physicochemical and Environmental Factors. **Environ Health Perspect,** v. 114, n. 2, p. 165-172, 2006.

HEYES, C. D.;KOBITSKI,A. Y.;BREUS, V. V.; NIENHAUS, G. U.Effect of the shell on the blinking statistics of core-shell quantum dots: A single-particle fluorescence study. **Phys. Rev. B,** v. 75, n. 12, p. 125431, 2007.

HINES, M.; GUYOT-SIONNEST, P. Synthesis and Characterization of Strongly Luminescing ZnS-Capped CdSe Nanocrystals. **J Phys Chem,** v. 100, n. 2, p. 468-471, 1996.

HU, Z. RAMÍREZ, D. J. E., CERVERA, B. E. H., OSKAM, G., SEARSON, P. C. Synthesis of ZnO Nanoparticles in 2-Propanol by Reaction with Water. **J Phys Chem B,** v. 109, n. 22, p. 11209-11214, 2005a.

HU, Z., SANTOS, J. F. H., OSKAM, G., SEARSON, P. C. Influence of the reactant concentrations on the synthesis of ZnO nanoparticles. **J Colloid Interface Sci,** v. 288, n. 1, p. 313-316, 2005b.

HU, Z.; OSKAM, G.; SEARSON, P. C. Influence of solvent on the growth of ZnO nanoparticles. **J Colloid Interface Sci,** v. 263, n. 2, p. 454-460, 2003.

HUYNH, N. T.; PASSIRANI, C.; SAULNIER, P.; BENOIT, J. P. Lipid nanocapsules: A new platform for nanomedicine. **Int J Pharm,** v. 379, n. 2, p. 201-209, 2009.

HYUN, B.-R.; CHEN, H.; REY, D. A.; WISE, F. W.; BATT, C. A. Near-Infrared Fluorescence Imaging with Water-Soluble Lead Salt Quantum Dots. **J Phys Chem B,** v. 111, n. 20, p. 5726-5730, 2007.

HYUN, H.;PARK, M. H.; OWENS, E. A.; WADA, H.; HENARY, M.; HANDGRAAF, H. J.; VAHRMEIJER, A. L.; FRANGIONI, J. V.; CHOI, H. S. Structure-inherent targeting of near-infrared fluorophores for parathyroid and thyroid gland imaging. **Nat Med,** v. 21, n. 2, p. 192-197, 2015.

IOANNOU, D.; GRIFFIN, D. K. Nanotechnology and molecular cytogenetics: the future has not yet arrived. **Nano Revs,** v. 1, p. 10.3402/, 2010.

ISNAENI; KIM, K. H.; NGUYEN, D. L.; LIM, H.;NGA, P. T.; CHO, Y.-H.Shell layer dependence of photoblinking in CdSe/ZnSe/ZnS quantum dots. **Appl Phys Lett,** v. 98, n. 1, p. 012109-3, 2011.

JAISWAL, J. K.;MATTOUSSI, H.; MAURO, J. M.; SIMON, S. M. Long-term multiple color imaging of live cells using quantum dot bioconjugates. **Nat Biotech,** v. 21, n. 1, p. 47-51, 2003.

JIA, Z.; MISRA, R. D. K. Tunable ZnO quantum dots for bioimaging: synthesis and photoluminescence. **Mater Technol,** v. 28, n. 4, p. 221-227, 2013.

JIN, S.;HU, Y.; GU, Z.;LIU, L.; WU, H.-C.Application of Quantum Dots in Biological Imaging. **J Nanomater,** v. 2011, p. 13, 2011.

JOSHI, B. P.; WANG, T. D. Exogenous Molecular Probes for Targeted Imaging in Cancer: Focus on Multi-modal Imaging. **Cancers,** v. 2, n. 2, p. 1251-1287, 2010.

KIRCHNER, C.; LIEDL, T.; KUDERA, S.; PELLEGRINO, T.; MUÑOZ JAVIER, A.; GAUB, H. E.; STÖLZLE, S.; FERTIG, N.; PARAK, W. J.Cytotoxicity of Colloidal CdSe and CdSe/ZnS Nanoparticles. **Nano Lett,** v. 5, n. 2, p. 331-338, 2005.

KOBAYASHI, K.; WEI, J.;IIDA, R.;IJIRO, K.;NIIKURA, K. Surface engineering of nanoparticles for therapeutic applications. **Polym J,** v. 46, n. 8, p. 460-468, 2014.

KUMAR, S.; SAHARE, P. D. Observation of band gap and surface defects of ZnO nanoparticles synthesized via hydrothermal route at different reaction temperature. **Opt Commun,** v. 285, n. 24, p. 5210-5216, 2012.

KWON, S. R. C. A. G. S. Polymeric Micelles for Drug Delivery. **Curr Pharm Des,** v. 12, n. 36, p. 4669-4684, 2006.

LAMPRECHT, A. Nanomedicines in gastroenterology and hepatology. **Nat Rev Gastroenterol Hepatol,** v. 12, n. 4, p. 195-204, 2015.

LI, L.; DAOU,T. J.; TEXIER, I.;CHI, T. T. K.;LIEM, N. Q.;REISS, P. Highly Luminescent CuInS2/ZnS Core/Shell Nanocrystals: Cadmium-Free Quantum Dots for In Vivo Imaging. **Chem Mater,** v. 21, n. 12, p. 2422-2429, 2009.

LI, S., SUN, Z., LI, R., DONG, M., ZHANG, L., QI, W., ZHANG, X., WANG, H.ZnO Nanocomposites Modified by Hydrophobic and Hydrophilic Silaneswith Dramatically Enhanced TunableFluorescence and Aqueous Ultrastabilitytoward Biological Imaging Applications. **Sci Rep,** v. 5, p. 8475:1-8, 2015.

LIU, Y.;AI, K.; YUAN, Q.; LU, L. Fluorescence-enhanced gadolinium-doped zinc oxide quantum dots for magnetic resonance and fluorescence imaging. **Biomaterials,** v. 32, n. 4, p. 1185-1192, 2011.

LORENZ, C.;EMMERLING, A.; FRICKE, J.; SCHMIDT, T.; HILGENDOR, M.; SPANHEL, L.; MÜLLER, G.Aerogels containing strongly photoluminescing zinc oxide nanocrystals1. **J Non Cryst Solids,** v. 238, n. 1–2, p. 1-5, 1998.

LUO, J.; ZHAO, S.; WU, P.; ZHANG, K.; PENG, C.;ZHENG, S. Synthesis and characterization of new Cd-doped ZnO/ZnS core-shell quantum dots with tunable and highly visible photoluminescence. **J Mater Chem C,** v. 3, n. 14, p. 3391-3398, 2015.

MAEDA, H. Tumor-Selective Delivery of Macromolecular Drugs via the EPR Effect: Background and Future Prospects. **Bioconjug Chem,** v. 21, n. 5, p. 797-802, 2010.

MANAIA, E. B., KAMINSKI, R. C. K., CAETANO, B.L., BRIOIS, V., CHIAVACCI, L. A., BOURGAUX, C. Surface modified Mg-doped ZnO QDs for biological imaging.**Eur J Nanomed**, v. 7,p. 109-120 , 2015.

MATSUMURA, Y.; MAEDA, H. A New Concept for Macromolecular Therapeutics in Cancer Chemotherapy: Mechanism of Tumoritropic Accumulation of Proteins and the Antitumor Agent Smancs. **Cancer Res,** v. 46, n. 12 Part 1, p. 6387-6392, 1986.

MOUSSA, H.; MERLIN, C.; DEZANET, C.; BALAN, L.; MEDJAHDI, G.; BEN-ATTIA, M.; SCHNEIDER, R. Trace amounts of Cu2+ ions influence ROS production and cytotoxicity of ZnO quantum dots. **J Hazard Mater,** v. 304, p. 532-542, 2016.

MOUSSODIA, R.-O, BALAN, L., MERLIN, C.,MUSTIN, C., SCHNEIDER, R. Biocompatible and stable ZnO quantum dots generated by functionalization with siloxane-core PAMAM dendrons. **J Mater Chem**, v. 20, p. 1147-1155, 2010.

MULDER, W. J.;KOOLE, R.; BRANDWIJK, R. J.; STORM, G.; CHIN, P. T.; STRIJKERS, G. J.; DE MELLO DONEGÁ, C.; NICOLAY, K.; GRIFFIOEN, A. W. Quantum Dots with a Paramagnetic Coating as a Bimodal Molecular Imaging Probe. **Nano Lett,** v. 6, n. 1, p. 1-6, 2006.

MURA, S.; NICOLAS, J.; COUVREUR, P. Stimuli-responsive nanocarriers for drug delivery. **Nat Mater,** v. 12, n. 11, p. 991-1003, 2013.

MUTHU, M. S.; LEONG, D. T.; MEI, L.; FENG, S. S.Nanotheranostics - Application and Further Development of Nanomedicine Strategies for Advanced Theranostics. **Theranostics**, v. 4, n. 6, p. 660-677, 2014.

NANODIODE, 2015. Disponível em: <http://en.rusnano.com/upload/OldNews/Files/33619/current.gif>. Acesso em: 30 mar.2016.

NICOLAS, J.; MURA, S.; BRAMBILLA, D.; MACKIEWICZ, N.; COUVREUR, P. Design, functionalization strategies and biomedical applications of targeted biodegradable/biocompatible polymer-based nanocarriers for drug delivery. **Chem Soc Rev,** v. 42, n. 3, p. 1147-1235, 2013.

NOEI, H., JIN, L., QIU, H., XU, M., GAO, Y., ZHAO, J., KAUER, M., WÖLL, C., MUHLER, M., WANG, Y.Vibrational spectroscopic studies on pure and metal-covered metal oxide surfaces.**Phys Status Solidi B Basic Solid State Phys**, v. 250, n. 6, p. 1204-1221, 2013.

NORBERG, N. S.; KITTILSTVED, K. R.; AMONETTE, J. E.; KUKKADAPU, R. K.; SCHWARTZ, D. A.; GAMELIN, D. R. Synthesis of Colloidal Mn2+:ZnO Quantum Dots and High-TC Ferromagnetic Nanocrystalline Thin Films. **J Am Chem Soc,** v. 126, n. 30, p. 9387-9398, 2004.

OH, E.; LIU, R.; NEL, A.; GEMILL, K. B.; BILAL, M.; COHEN, Y.; MEDINTZ, I. L. Meta-analysis of cellular toxicity for cadmium-containing quantum dots. **Nat Nanotechnol,** v. advance online publication, 2016.

OWENS III, D. E.; PEPPAS, N. A. Opsonization, biodistribution, and pharmacokinetics of polymeric nanoparticles. **Int J Pharm,** v. 307, n. 1, p. 93-102, 2006.

PAN, D.;WANG, Q.; JIANG, S.; JI, X.; AN, L. Synthesis of Extremely Small CdSe and Highly Luminescent CdSe/CdS Core–Shell Nanocrystals via a Novel Two-Phase Thermal Approach. **Adv Mater,** v. 17, n. 2, p. 176-179, 2005.

PAN, J.;WAN, D.; BIAN, Y.; GUO, Y.; JIN, F.; WANG, T.; GONG, T. Reduction of nonspecific binding for cellular imaging using quantum dots conjugated with vitamin E. **AIChE J,** v. 60, n. 5, p. 1591-1597, 2014.

PAN, Z.-Y.;LIANG, J.; ZHENG, Z. Z.; WANG, H. H.; XIONG, H. M. The application of ZnO luminescent nanoparticles in labeling mice. **Contrast Media Mol Imaging,** v. 6, n. 4, p. 328-330, 2011.

PANSARE, V.; HEJAZI, S.; FAENZA, W.; PRUD'HOMME, R. K.. Review of Long-Wavelength Optical and NIR Imaging Materials: Contrast Agents, Fluorophores and Multifunctional Nano Carriers. **Chem Mater.,** v. 24, n. 5, p. 812-827, 2012.

PAPAGIANNAROS, A.; LEVCHENKO, T.; HARTNER, W.; MONGAYT, D.; TORCHILIN, V. Quantum dots encapsulated in phospholipid micelles for imaging and quantification of tumors in the near-infrared region. **Nanomedicine,** v. 5, n. 2, p. 216-224, 2009.

PATTNI, B. S.; CHUPIN, V. V.; TORCHILIN, V. P. New Developments in Liposomal Drug Delivery. **Chemical Reviews,** v. 115, n. 19, p. 10938-10966, 2015.

PELTIER, S.; OGER, J. M.; LAGARCE, F.; COUET, W.; BENOÎT, J. P. Enhanced Oral Paclitaxel Bioavailability After Administration of Paclitaxel-Loaded Lipid Nanocapsules. **Pharm Res,** v. 23, n. 6, p. 1243-1250, 2006.

PENET, M.-F.; MIKHAYLOVA, M.; LI, C.; KRISHNAMACHARY, B.; GLUNDE, K.; PATHAK, A. P.; BHUJWALLA, Z. M.. Applications of molecular MRI and optical imaging in cancer. **Future Med Chem,** v. 2, n. 6, p. 975-988, 2010.

PRADHAN, A. K.; MUNDLE, R. M.; SANTIAGO, K.; SKUZA, J. R.; XIAO, B.; SONG, K. D.; BAHOURA, M.; CHEAITO, R.; HOPKINS, P. E. Extreme tunability in aluminum doped Zinc Oxide plasmonic materials for near-infrared applications. **Sci. Rep.,** v. 4, p. 1-6, 2014.

PURI, A.; LOOMIS, K.; SMITH, B.; LEE, J. H.; YAVLOVICH, A.; HELDMAN, E.; BLUMENTHAL, R.. Lipid-Based Nanoparticles as Pharmaceutical Drug Carriers: From Concepts to Clinic. **Crit Rev Ther Drug Carrier Syst.,** v. 26, n. 6, p. 523-580, 2009.

RABANEL, J. M.;AOUN, V.; ELKIN, I.; MOKHTAR, M.; HILDGEN, P. Drug-Loaded Nanocarriers: Passive Targeting and Crossing of Biological Barriers. **Curr Med Chem,** v. 19, n. 19, p. 3070-3102, 2012.

RATH, T.; KUNERT, B.; RESEL, R.; FRITZ-POPOVSKI, G.; SAF, R.; TRIMMEL, G. Investigation of Primary Crystallite Sizes in Nanocrystalline ZnS Powders: Comparison of Microwave Assisted with Conventional Synthesis Routes. **Inorg Chem,** v. 47, n. 8, p. 3014-3022, 2008.

REISS, P. ZnSe based colloidal nanocrystals: synthesis, shape control, core/shell, alloy and doped systems. **New J Chem,** v. 31, n. 11, p. 1843-1852, 2007.

REISS, P.; PROTIÈRE, M.; LI, L. Core/Shell Semiconductor Nanocrystals. **Small,** v. 5, n. 2, p. 154-168, 2009.

SCHMIDT, T.; MÜLLER, G.; SPANHEL, L. Activation of 1.54 μm Er3+ Fluorescence in Concentrated II−VI Semiconductor Cluster Environments. **Chem Mater,** v. 10, n. 1, p. 65-71, 1998.

SCHWARTZ, D. A.;NORBERG, N. S.; NGUYEN, Q. P.; PARKER, J. M.; GAMELIN, D. R. Magnetic Quantum Dots: Synthesis, Spectroscopy, and Magnetism of Co2+- and Ni2+-Doped ZnO Nanocrystals. **J Am Chem Soc,** v. 125, n. 43, p. 13205-13218, 2003.

SHARMA, S.; VYAS, R.; SHARMA, N.; SINGH, V.; SINGH, A.; KATARIA, V.; GUPTA, B. K.; VIJAY, Y. K.Highly efficient green light harvesting from Mg doped ZnO nanoparticles: Structural and optical studies. **J Alloys Compd,** v. 552, p. 208-212, 2013.

SIEKMANN, B.; WESTESEN, K. Sub-micron sized parenteral carrier systems based on solid lipid **Pharm. Pharmacol. Lett.,** v. 1, p. 123-126, 1992.

SKANDRANI, N.; BARRAS, A.; LEGRAND, D.; GHARBI, T.; BOULAHDOUR, H.; BOUKHERROUB, R.. Lipid nanocapsules functionalized with polyethyleneimine for plasmid DNA and drug co-delivery and cell imaging. **Nanoscale,** v. 6, n. 13, p. 7379-7390, 2014.

SMITH, A. M.; DUAN, H.; MOHS, A. M.; NIE, S. Bioconjugated quantum dots for in vivo molecular and cellular imaging. **Adv Drug Deliv Rev,** v. 60, n. 11, p. 1226-1240, 2008.

SPANHEL, L.; ANDERSON, M. A. Semiconductor clusters in the sol-gel process: quantized aggregation, gelation, and crystal growth in concentrated zinc oxide colloids. **J Am Chem Soc,** v. 113, n. 8, p. 2826-2833, 1991.

SPERLING, R. A.; PARAK, W. J. Surface modification, functionalization and bioconjugation of colloidal inorganic nanoparticles. **Philos Trans R Soc London, Ser A,** v. 368, n. 1915, p. 1333-1383, 2010.

STOCKHOFE, K.; POSTEMA, J. M.; SCHIEFERSTEIN, H.; ROSS, T. L. Radiolabeling of Nanoparticles and Polymers for PET Imaging. **Pharmaceuticals,** v. 7, n. 4, p. 392–418, 2014.

SU, Y.; HE, Y.; LU, H.; SAI, L.; LI, Q.; LI, W.; WANG, L.; SHEN, P.; HUANG, Q.; FAN, C. The cytotoxicity of cadmium based, aqueous phase – Synthesized, quantum dots and its modulation by surface coating. **Biomaterials,** v. 30, n. 1, p. 19-25, 2009.

SUN, L.-W.; SHI, H.-Q.; LI, W.-N.; XIAO, H.-M.; FU, S.-Y.; CAO, X.-Z.; LI, Z.-X.. Lanthanum-doped ZnO quantum dots with greatly enhanced fluorescent quantum yield. **J Mater Chem,** v. 22, n. 17, p. 8221-8227, 2012.

TANG, J.;KEMP, K. W.; HOOGLAND, S.; JEONG, K. S.; LIU, H.; LEVINA, L.; FURUKAWA, M.; WANG, X.; DEBNATH, R.; CHA, D.; CHOU, K. W.; FISCHER, A.; AMASSIAN, A.; ASBURY, J. B.; SARGENT, E. H. Colloidal-quantum-dot photovoltaics using atomic-ligand passivation. **Nat Mater,** v. 10, n. 10, p. 765-771, 2011.

TERRENO, E.; DASTRÙ, W.; DELLI CASTELLI, D.; GIANOLIO, E.; GENINATTI CRICH, S.; LONGO, D.; AIME, S. Advances in Metal-Based Probes for MR Molecular Imaging Applications. **Curr Med Chem,** v. 17, n. 31, p. 3684-3700, 2010.

TOKUMOTO, M. S., BRIOS, V.; SANTILLI, C. V.; PULCINELLI, S. H.Preparation of ZnO Nanoparticles: Structural Study of the Molecular Precursor. **J Solgel Sci Technol,** v. 26, n. 1-3, p. 547-551, 2003a.

TOKUMOTO, M. S.,PULCINELLI, S. H., SANTILLI, C. V. BRIOIS, V. Catalysis and Temperature Dependence on the Formation of ZnO Nanoparticles and of Zinc Acetate Derivatives Prepared by the Sol−Gel Route. **J Phys Chem B,** v. 107, n. 2, p. 568-574, 2003b.

TORCHILIN, V. P. Recent advances with liposomes as pharmaceutical carriers. **Nat Rev Drug Discov,** v. 4, n. 2, p. 145-160, 2005.

VIGLIANTI, B. L.; PONCE, A. M.; MICHELICH, C. R.; YU, D.; ABRAHAM, S. A.; SANDERS, L.; YARMOLENKO, P. S.; SCHROEDER, T.; MACFALL, J. R.; BARBORIAK, D. P.; COLVIN, O. M.; BALLY, M. B.; DEWHIRST, M.Chemodosimetry of in vivo tumor liposomal drug concentration using MRI. **Magn Reson Med,** v. 56, n. 5, p. 1011-1018, 2006.

WANG, X.; REN, X.; KAHEN, K.; HAHN, M. A.; RAJESWARAN, M.; MACCAGNANO-ZACHER, S.; SILCOX, J.; CRAGG, G. E.; EFROS, A. L.; KRAUSS, T. D. Non-blinking semiconductor nanocrystals. **Nature,** v. 459, n. 7247, p. 686-689, 2009.

WANG, Y. S.; THOMAS, P. J.; O'BRIEN, P. Optical properties of ZnO nanocrystals doped with Cd, Mg, Mn, and Fe ions. **J Phys Chem B,** v. 110, n. 43, p. 21412-21415, 2006.

WEI, X.; WANG, W.; CHEN, K. ZnO:Er,Yb,Gd Particles Designed for Magnetic-Fluorescent Imaging and Near-Infrared Light Triggered Photodynamic Therapy. **J Phys Chem CNanomater Interfaces,** v. 117, n. 45, p. 23716-23729, 2013.

WEISSLEDER, R. A clearer vision for in vivo imaging. **Nat Biotech,** v. 19, n. 4, p. 316-317, 2001.

WEN, C.-J.; ZHANG, L. W.; AL-SUWAYEH, S. A.; YEN, T. C.; FANG, J. Y. Theranostic liposomes loaded with quantum dots and apomorphine for brain targeting and bioimaging. **Int J Nanomedicine,** v. 7, p. 1599-1611, 2012.

WIECINSKI, P. N.; METZ, K. M.; KING HEIDEN, T. C.; LOUIS, K. M.; MANGHAM, A. N.; HAMERS, R. J.; HEIDEMAN, W.; PETERSON, R. E.; PEDERSEN, J. A. Toxicity of Oxidatively Degraded Quantum Dots to Developing Zebrafish (Danio rerio). **Environ Sci Technol.,** v. 47, n. 16, p. 9132-9139, 2013.

WOLSKA, E.;KASZEWSKI, J.; KIEŁBIK, P.; GRZYB, J.; GODLEWSKI, M.M.; GODLEWSKI, M.. Rare earth activated ZnO nanoparticles as biomarkers. **Opt Mater,** v. 36, n. 10, p. 1655-1659, 2014.

WOOD, A.; GIERSIG, M.; HILGENDORFF, M.; VILAS-CAMPOS, A.; LIZ-MARZÁN, L. M.; MULVANEY, P.. Size Effects in ZnO: The Cluster to Quantum Dot Transition. **Aust J Chem,** v. 56, n. 10, p. 1051-1057, 2003.

WU, Y. L.;FU, S.; TOK, A. I.; ZENG, X. T.; LIM, C. S.; KWEK, L. C.; BOEY, F. C. A dual-colored bio-marker made of doped ZnO nanocrystals. **Nanotechnology,** v. 19, n. 34, p.1-9, 2008.

XIONG, H.-M. XU, Y.; REN, Q. G.; XIA, Y. Y. Stable Aqueous ZnO@Polymer Core−Shell Nanoparticles with Tunable Photoluminescence and Their Application in Cell Imaging. **J Am Chem Soc,** v. 130, n. 24, p. 7522-7523, 2008.

XIONG, H.-M. Photoluminescent ZnO nanoparticles modified by polymers. **J Mater Chem,** v. 20, n. 21, p. 4251-4262, 2010.

YAN, C.; TANG, F.; LI, L.; LI, H.; HUANG, X.; CHEN, D.; MENG, X.; REN, J. Synthesis of Aqueous CdTe/CdS/ZnS Core/shell/shell Quantum Dots by a Chemical Aerosol Flow Method. **Nanoscale Res Lett,** v. 5, n. 1, p. 189-194, 2009.

YANG, J.;YAO, M. H.; WEN, L.; SONG, J. T.; ZHANG, M. Z.; ZHAO, Y. D.; LIU, B. Multifunctional quantum dot-polypeptide hybrid nanogel for targeted imaging and drug delivery. **Nanoscale,** v. 6, n. 19, p. 11282-11292, 2014.

YANG, Y.;JIN, Y.; HE, H.; WANG, Q.; TU, Y.; LU, H.; YE, Z.Dopant-Induced Shape Evolution of Colloidal Nanocrystals: The Case of Zinc Oxide. **J Am Chem Soc,** v. 132, n. 38, p. 13381-13394, 2010.

YANG Y., LV, S-Y. YU, B., XU, S., SHEN, J., ZHAO, T., ZHANG, H. Hepatotoxicity assessment of Mn-doped ZnS quantum dots after repeated administration in mice. **Int J Nanomedicine,** v. 10, p. 5787-5796, 2015.

YHEE, J. Y.; LEE, S.; KIM, K. Advances in targeting strategies for nanoparticles in cancer imaging and therapy. **Nanoscale,** v. 6, n. 22, p. 13383-13390, 2014.

YIN, Q.;JIN, X.;YANG, G.;JIANG, C.;SONGA, Z.; SUN, G. Biocompatible folate-modified Gd3+/Yb3+-doped ZnO nanoparticles for dualmodal MRI/CT imaging. **RSC Adv,** v. 4, n. 96, p. 53561-53569, 2014.

YOUSEFI, R.; ZAK, A. K.; JAMALI-SHEINI, F. Growth, X-ray peak broadening studies, and optical properties of Mg-doped ZnO nanoparticles. **Mater Sci Semicond Process,** v. 16, n. 3, p. 771-777, 2013.

YU, M. K.; PARK, J.; JON, S. Targeting Strategies for Multifunctional Nanoparticles in Cancer Imaging and Therapy. **Theranostics**,v. 2, n. 1, p. 3-44, 2012.

LV, Y., XIAO, W. LI, W., XUE, J., DING, J. Controllable synthesis of ZnO nanoparticles with high intensity visible photoemission and investigation of its mechanism. **Nanotechnology,** v. 24, n. 17, p. 175702:1-10, 2013.

ZHANG, Z.H., WANG, X., XU, J.B., MULLER, S., RONNING, C. & LI., Q. Evidence of intrinsic ferromagnetism in individual dilute magnetic semiconductor nanostructures. **Nature Nanotech**. v.4, p. 523-527 , 2009.

ZHANG, H-J., XIONG, H-M., REN, Q-G., XIA, Y-Y., KONG, J-L. ZnO@silica core–shell nanoparticles with remarkable luminescence andstability in cell imaging. **J Mater Chem**, v. 22, p. 13159-13165, 2012.

ZHANG, Z-Y., XU, Y-D., MA, Y-Y., QIU, L-L., WANG, Y., KONG, J-L., XIONG, H-M.Biodegradable ZnO@polymer Core–Shell Nanocarriers: pH-TriggeredRelease of Doxorubicin In Vitro. **Angew Chem Int Ed Engl**, v. 52, p. 4127-4131, 2013.

ZHANG, Y.; HUANG, Y.; LI, S. Polymeric Micelles: Nanocarriers for Cancer-Targeted Drug Delivery. **AAPS PharmSciTech**, New York**,** v. 15, n. 4, p. 862-871, 2014.

ZHAO, L.-H.; ZHANG, R.; ZHANGA, J.;SUN, S.-Q. Synthesis and characterization of biocompatible ZnO nanoparticles. **CrystEngComm,** v. 14, n. 3, p. 945-950, 2012.

ZHOU, R.;LI, M.; WANG, S.; WU, P.; WU, L.; HOU, X. Low-toxic Mn-doped ZnSe@ZnS quantum dots conjugated with nano-hydroxyapatite for cell imaging. **Nanoscale,** v. 6, n. 23, p. 14319-14325, 2014.

## II.4. REFERENCES

BANCOS, S.; STEVENS, D. L.; TYNER, K. M. Effect of silica and gold nanoparticles on macrophage proliferation, activation markers, cytokine production, and phagocytosis in vitro. **Int J Nanomedicine,** v. 10, p. 183-206, 2015.

BRIOIS, V.; SERRINI, P.; CHIAVACCI, L.; PULCINELLI, S. H.;SANTILLI, C. V.EXAFS spectroscopy of nanocrystalline materials. In: NETWORK, T. R. (Ed.). **Recent Research and Development of Non-Crystalline Solids**. Kerala, India, v.1, 2001. p.21-35. ISBN 81-7895-028-6.

BRUS, L. E. A simple model for the ionization potential, electron affinity, and aqueous redox potentials of small semiconductor crystallites. **J Chem Phys,** v. 79, n. 11, p. 5566-5571, 1983.

CHEMIN, C.;PÉAN, J. M.; BOURGAUX, C.; PABST, G.; WÜTHRICH, P.; COUVREUR, P.; OLLIVON, M.Supramolecular organization of S12363-liposomes prepared with two different remote loading processes. **Biochim Biophys Acta,** v. 1788, n. 5, p. 926-935, 2009.

CHUKWUOCHA, E.; ONYEAJU, M.; HARRY, T. Theoretical Studies on the Effect of Confinement on Quantum Dots Using the Brus Equation. **World Journal of Condensed Matter Physics,** v. 2, n. 2, p. 96-100, 2012.

CRAIEVICH, A. F. **Handbook of Sol-Gel Science and Technology**;Norwell: Sakka, S., Almeida, R., Eds., 2005. vol.2, chapter II, p 161-189.

CROSBY, G. A.; DEMAS, J. N. Measurement of photoluminescence quantum yields. Review. **J Phys Chem,** v. 75, n. 8, p. 991-1024, 1971.

DONG, Y.-D.; BOYD, B. J. Applications of X-ray scattering in pharmaceutical science. **Int J Pharm,** v. 417, n. 1–2, p. 101-111, 2011.

GRUNWALDT, J.-D.; BAIKER, A. In situ spectroscopic investigation of heterogeneous catalysts and reaction media at high pressure. **Phys Chem Chem Phys,** v. 7, n. 20, p. 3526-3539, 2005.

INOBE, T.;TAKAHASHI, K.; MAKI, K.; ENOKI, S.; KAMAGATA, K.; KADOOKA, A.; ARAI, M.; KUWAJIMA, K. Asymmetry of the GroEL-GroES Complex under Physiological Conditions as Revealed by Small-Angle X-Ray Scattering. **Biophys J,** v. 94, n. 4, p. 1392-1402, 2008.

KOHLBRECHER, J.; BRESSLER, I. **SASfit**. Paul Scherrer Institut, Villigen, Switzerland. 0.94.1 2014.

LEPELTIER, E., BOURGAXU, C., COUVREUR P. Nanoprecipitation and the "Ouzo effect": Application to drug delivery devices. **Adv Drug Deliv Rev**, v.71, p. 86-97, 2014.

MANAIA, E. B.;KAMINSKI, R. C.; DE OLIVEIRA, A. G.; CORRÊA, M. A.; CHIAVACCI, L. A. Multifunction hexagonal liquid-crystal containing modified surface $TiO_2$ nanoparticles and terpinen-4-ol for controlled release. **Int J Nanomedicine,** v. 10, p. 811-819, 2015.

MEULENKAMP, E. A. Synthesis and Growth of ZnO Nanoparticles. **J Phys Chem B,** v. 102, n. 29, p. 5566-5572, 1998.

MULET, X.; BOYD, B. J.; DRUMMOND, C. J. Advances in drug delivery and medical imaging using colloidal lyotropic liquid crystalline dispersions. **J Colloid Interface Sci,** v. 393, p. 1-20, 2013.

NASCIMENTO, T. L.; HILLAIREAU, H.; NOIRAY, M.; BOURGAUX, C.; ARPICCO, S.; PEHAU-ARNAUDET, G.; TAVERNA, M.; COSCO, D.; TSAPIS, N.; FATTAL, E.Supramolecular Organization and siRNA Binding of Hyaluronic Acid-Coated Lipoplexes for Targeted Delivery to the CD44 Receptor. **Langmuir,** v. 31, n. 41, p. 11186-11194, 2015.

NEDELIJKOVIC, J. M.; PATEL, R. C.;KAUFMAN, P.;JOYCE-PRUDEN, C.;O'LEARY, N. Synthesis and optical properties of quantum-sized metal sulfide particles in aqueous solution.**J Chem Educ,** v. 70, n. 4, p. 342, 1993.

PETOUKHOV, M. V.; SVERGUN, D. I. Applications of small-angle X-ray scattering to biomacromolecular solutions. **Int J Biochem Cell Biol,** v. 45, n. 2, p. 429-437, 2013.

SPANHEL, L.; ANDERSON, M. A. Semiconductor clusters in the sol-gel process: quantized aggregation, gelation, and crystal growth in concentrated zinc oxide colloids. **J Am Chem Soc,** v. 113, n. 8, p. 2826-2833, 1991.

SUN, L.-W.; SHI, H.-Q.; LI, W.-N.; XIAO, H.-M.; FU, S.-Y.; CAO, X.-Z.; LI, Z.-X.. Lanthanum-doped ZnO quantum dots with greatly enhanced fluorescent quantum yield. **J Mater Chem,** v. 22, n. 17, p. 8221-8227, 2012.

WEST, A. R. **Solid State Chemistry and Its Applications**. New York: John Wiley and Sons, 1992.

WILLIAMS, D. B., CARTER, C. B. **Transmission Electron Microscopy. A Textbook for Materials Science**. New Your: Springer Science+Business Media, 2009. p. 49.

YANO, J.; YACHANDRA, V. K. X-ray absorption spectroscopy. **Photosynthesis Research,** v. 102, n. 2-3, p. 241-254, 2009.

## III.5. REFERENCES

BIAN, S.-W.; MUDUNKOTUWA, I. A.; RUPASINGHE, T.; GRASSIAN, V. H.Aggregation and Dissolution of 4 nm ZnO Nanoparticles in Aqueous Environments: Influence of pH, Ionic Strength, Size, and Adsorption of Humic Acid. **Langmuir,** v. 27, n. 10, p. 6059-6068, 2011.

BRIOIS, V. GIORGETTI, C.H.; BAUDELET,F.;BLANCHANDIN, S.; TOKUMOTO, M. S.; PULCINELLI,S. H.; SANTILLI, C. V. Dynamical Study of ZnO Nanocrystal and Zn-HDS Layered Basic Zinc Acetate Formation from Sol−Gel Route. **J Phys Chem CNanomater Interfaces,** v. 111, n. 8, p. 3253-3258, 2007.

BRUS, L. E. A simple model for the ionization potential, electron affinity, and aqueous redox potentials of small semiconductor crystallites. **J Chem Phys,** v. 79, n. 11, p. 5566-5571, 1983.

CAETANO, B. L. SANTILLI, C. V.; MENEAU, F.; BRIOIS, V.; PULCINELLI, S. H. In Situ and Simultaneous UV−vis/SAXS and UV−vis/XAFS Time-Resolved Monitoring of ZnO Quantum Dots Formation and Growth. **J Phys Chem CNanomater Interfaces,** v. 115, n. 11, p. 4404-4412, 2011.

CASSETTE, E.;PONS, T.;BOUET, C.; HELLE, M.;BEZDETNAYA, L.; MARCHAL, F.;DUBERTRET, B.Synthesis and Characterization of Near-Infrared Cu−In−Se/ZnS Core/Shell Quantum Dots for In vivo Imaging. **Chem Mater,** v. 22, n. 22, p. 6117-6124, 2010.

CHEN, O.;ZHAO, J.; CHAUHAN, V. P.; CUI, J.; WONG, C.; HARRIS, D. K.; WEI, H.; HAN, H. S.; FUKUMURA, D.; JAIN, R. K.; BAWENDI, M. G. Compact high-quality CdSe–CdS core–shell nanocrystals with narrow emission linewidths and suppressed blinking. **Nat Mater,** v. 12, n. 5, p. 445-451, 2013.

CURCIO, A. L.; BERNARDI, M. I. B.; MESQUITA, A. Local structure and photoluminescence properties of nanostructured Zn1-xMnxS material. **Phys Status Solidi Rapid Res Lett.,** v. 12, n. 12, p. 1367-1371, 2015.

DABBOUSI, B. O.; RODRIGUEZ-VIEJO, J.; MIKULEC, F. V.; HEINE, J. R.; MATTOUSSI, H.; OBER, R.; JENSEN, K. F.; BAWENDI, M. G. (CdSe)ZnS Core−Shell Quantum Dots: Synthesis and Characterization of a Size Series of Highly Luminescent Nanocrystallites. **J Phys Chem B,** v. 101, n. 46, p. 9463-9475, 1997.

DAVID, C. A.;GALCERAN, J.;REY-CASTRO, C.;PUY, J.;COMPANYS, E.;SALVADOR, J.;MONNÉ, J.;WALLACE, R.;VAKOUROV, A.Dissolution Kinetics and Solubility of ZnO Nanoparticles Followed by AGNES. **J Phys Chem CNanomater Interfaces,** v. 116, n. 21, p. 11758-11767, 2012.

GENG, J.; LIU, B.; XU, L.; HU, F. N.; ZHU, J. J. Facile Route to Zn-Based II−VI Semiconductor Spheres, Hollow Spheres, and Core/Shell Nanocrystals and Their Optical Properties. **Langmuir,** v. 23, n. 20, p. 10286-10293, 2007.

GHOSH CHAUDHURI, R.; PARIA, S. Core/Shell Nanoparticles: Classes, Properties, Synthesis Mechanisms, Characterization, and Applications. **Chem Rev,** v. 112, n. 4, p. 2373-2433, 2011.

GUINIER, A.; FOURNET, G. **Small Angle Scattering of X-rays**. New-York: Wiley, 1955.

ISNAENI; KIM, K. H.; NGUYEN, D. L.; LIM, H.;NGA, P. T.; CHO, Y.-H. Shell layer dependence of photoblinking in CdSe/ZnSe/ZnS quantum dots. **Appl Phys Lett,** v. 98, n. 1, p. 012109-3, 2011.

JIA, Z.; MISRA, R. D. K. Tunable ZnO quantum dots for bioimaging: synthesis and photoluminescence. **Mater Technol,** v. 28, n. 4, p. 221-227, 2013.

LIM, J. H.;KANG, C. K.;KIM, K. K.;PARK, I. K.;HWANG, D. K.;PARK, S. J. UV Electroluminescence Emission from ZnO Light-Emitting Diodes Grown by High-Temperature Radiofrequency Sputtering. **Adv Mater,** v. 18, n. 20, p. 2720-2724, 2006.

LIU, K.; SAKURAI, M.; AONO, M. ZnO-Based Ultraviolet Photodetectors. **Sensors (Basel, Switzerland),** v. 10, n. 9, p. 8604-8634, 2010.

LIU, L.;CHEN, Y.;GUO, T.;ZHU, Y.;SU, Y.;JIA, C.;WEI, M.;CHENG, Y.Chemical Conversion Synthesis of ZnS Shell on ZnO Nanowire Arrays: Morphology Evolution and Its Effect on Dye-Sensitized Solar Cell. **ACS Appl Mater Interfaces,** v. 4, n. 1, p. 17-23, 2011.

LUO, J.; ZHAO, S.; WU, P.; ZHANG, K.; PENG, C.;ZHENG, S. Synthesis and characterization of new Cd-doped ZnO/ZnS core-shell quantum dots with tunable and highly visible photoluminescence. **J Mater Chem C,** v. 3, n. 14, p. 3391-3398, 2015.

MATSUYAMA, K.; IHSAN, N.; IRIE, K.; MISHIMA, K.; OKUYAMA, T.; MUTO, H. Bioimaging application of highly luminescent silica-coated ZnO-nanoparticle quantum dots with biotin. **J Colloid Interface Sci,** v. 399, p. 19-25, 2013.

MEHTA, S. K.;KUMAR, S.; CHAUDHARY, S.; BHASIN, K. K.; GRADZIELSKI, M. Evolution of ZnS Nanoparticles via Facile CTAB Aqueous Micellar Solution Route: A Study on Controlling Parameters. **Nanoscale Res Lett,** v. 4, n. 1, p. 17-28, 2008.

MEULENKAMP, E. A. Size Dependence of the Dissolution of ZnO Nanoparticles. **J Phys Chem B,** v. 102, n. 40, p. 7764-7769, 1998.

MOUSSODIA, R.-O, BALAN, L., MERLIN, C.,MUSTIN, C., SCHNEIDER, R. Biocompatible and stable ZnO quantum dots generated by functionalization with siloxane-core PAMAM dendrons. **J Mater Chem**, v. 20, p. 1147-1155, 2010.

NAM, W.; LIM, Y. S.; SEO, W.-S.;CHO, H. K.;LEE, J. Y. Control of the shell structure of ZnO–ZnS core-shell structure. **J Nanopart Res,** v. 13, n. 11, p. 5825-5831, 2011.

PANDA, S. K.; DEV, A.; CHAUDHURI, S. Fabrication and luminescent properties of c-axis oriented ZnO-ZnS core-shell and ZnS nanorod arrays by sulfidation of aligned ZnO nanorod arrays. **J Phys Chem C Nanomater Interfaces,** v. 111, n. 13, p. 5039-5043, 2007.

REISS, P.; PROTIÈRE, M.; LI, L. Core/Shell Semiconductor Nanocrystals. **Small,** v. 5, n. 2, p. 154-168, 2009.

SADOLLAHKHANI, A.;KAZEMINEZHAD, I.;LU, J.;NUR, O.;HULTMAN, L.;WILLANDER, M. Synthesis, structural characterization and photocatalytic application of ZnO@ZnS core-shell nanoparticles. **RSC Adv,** v. 4, n. 70, p. 36940-36950, 2014.

SHARMA, M.; KUMAR, S.; PANDEY, O. P. Study of energy transfer from capping agents to intrinsic vacancies/defects in passivated ZnS nanoparticles. **J Nanopart Res,** v. 12, n. 7, p. 2655-2666, 2010.

SHARMA, S.; CHAWLA, S. Enhanced UV emission in ZnO/ZnS core shell nanoparticles prepared by epitaxial growth in solution. **Electronic Materials Letters,** v. 9, n. 3, p. 267-271, 2013.

SHUAI, X. M.; SHEN, W. Z. A Facile Chemical Conversion Synthesis of ZnO/ZnS Core/Shell Nanorods and Diverse Metal Sulfide Nanotubes. **J Phys Chem CNanomater Interfaces,** v. 115, n. 14, p. 6415-6422, 2011.

SOOKHAKIAN, M.; AMIN, Y. M.;BASIRUN, W. J.;TAJABADI, M. T.;KAMARULZAMAN, N. Synthesis, structural, and optical properties of type-II ZnO–ZnS core–shell nanostructure. **J Lumin,** v. 145, n. 0, p. 244-252, 2014.

THUY, U. T. D., LIEM, N. Q. Transition from type-I to type-II CdTe/CdS core/shell quantum dots synthesized in water at low temperature.**J Nanosci Nanotechnol,** v. 4, n. 4, p. 045010, 2013.

TOKUMOTO, M. S., BRIOS, V.; SANTILLI, C. V.; PULCINELLI, S. H. Preparation of ZnO Nanoparticles: Structural Study of the Molecular Precursor. **J Solgel Sci Technol,** v. 26, n. 1-3, p. 547-551, 2003.

VERMA, P.; PANDEY, A. C.; BHARGAVA, R. N. Synthesis and characterisation: Zinc oxide–sulfide nanocomposites. **Physica B Condens Matter,** v. 404, n. 21, p. 3894-3897, 2009.

WANG, X.; REN, X.; KAHEN, K.; HAHN, M. A.; RAJESWARAN, M.; MACCAGNANO-ZACHER, S.; SILCOX, J.; CRAGG, G. E.; EFROS, A. L.; KRAUSS, T. D. Non-blinking semiconductor nanocrystals. **Nature,** v. 459, n. 7247, p. 686-689, 2009a.

WANG, Y., GUO, Q., LIN, S., CHEN, B., ZHENG, D. Growth and properties of ZnO/ZnS core/shell nanostructures. **Journal of Physics: Conference Series,** v. 152, n. 1, p. 012018, 2009b.

WANG, L.;KANG, Y.;LIU, X.;ZHANG, S.;HUANG, W.;WANG, S.ZnO nanorod gas sensor for ethanol detection. **Sens Actuators B Chem,** v. 162, n. 1, p. 237-243, 2012.

WEST, A. R. **Solid State Chemistry and Its Applications**. New York: John Wiley and Sons 1992.

WU, D.; JIANG, Y.;YUAN, Y.;WU, J.;JIANG, K. ZnO–ZnS heterostructures with enhanced optical and photocatalytic properties. **J Nanopart Res,** v. 13, n. 7, p. 2875-2886, 2011.

XIONG, H.-M. Photoluminescent ZnO nanoparticles modified by polymers. **J Mater Chem,** v. 20, n. 21, p. 4251-4262, 2010.

XIONG, H.-X. ZnO Nanoparticles Applied to Bioimaging and Drug Delivery. **Adv Mater,** v. 25, n. 37, p. 5329-5335, 2013.

## IV.5. REFERENCES

BAGALKOT, V.;ZHANG, L.; LEVY-NISSENBAUM, E.; JON, S.; KANTOFF, P. W.; LANGER, R.; FAROKHZAD, O. C. Quantum Dot−Aptamer Conjugates for Synchronous Cancer Imaging, Therapy, and Sensing of Drug Delivery Based on Bi-Fluorescence Resonance Energy Transfer. **Nano Lett,** v. 7, n. 10, p. 3065-3070, 2007.

BRINKER, C. J.; SCHERER, G. W. **Sol-Gel Sciences. The Physics and Chemistry of Sol-Gel Processing.** San Diego: Academic Press, Inc, p. 908, 1990.

BRUS, L. Electronic wave functions in semiconductor clusters: experiment and theory. **J Phys Chem,** v. 90, n. 12, p. 2555-2560, 1986.

BUONSANTI, R.; MILLIRON, D. J. Chemistry of Doped Colloidal Nanocrystals. **Chem Mater,** v. 25, n. 8, p. 1305-1317, 2013.

CAETANO, B. L. SANTILLI, C. V.; MENEAU, F.; BRIOIS, V.; PULCINELLI, S. H. In Situ and Simultaneous UV−vis/SAXS and UV−vis/XAFS Time-Resolved Monitoring of ZnO Quantum Dots Formation and Growth. **J Phys Chem CNanomater Interfaces,** v. 115, n. 11, p. 4404-4412, 2011.

CHANG, E.;THEKKEK, N.; YU, W. W.; COLVIN, V. L.; DREZEK, R.. Evaluation of Quantum Dot Cytotoxicity Based on Intracellular Uptake. **Small,** v. 2, n. 12, p. 1412-1417, 2006.

COHN, A. W.; KITTILSTVED, K. R.; GAMELIN, D. R. Tuning the Potentials of "Extra" Electrons in Colloidal n-Type ZnO Nanocrystals via $Mg^{2+}$ Substitution. **J Am Chem Soc,** v. 134, n. 18, p. 7937-7943, 2012.

CRAIEVICH, A. F. **Handbook of Sol-Gel Science and Technology**. Norwell, MA: Kluwer Publishers, p.161-189, 2005.

DING, R.;XU, C.;GU, B.;SHI, Z.; WANG, H.;BA, L.;XIAO, Z. Effects of Mg Incorporation on Microstructure and Optical Properties of ZnO Thin Films Prepared by Sol-gel Method. **J Mater Sci Technol,** v. 26, n. 7, p. 601-604, 2010.

FELBIER, P.;YANG, J.;THEIS, J.;LIPTAK, R. W.;WAGNER, A.;LORKE, A.;BACHER, G.;KORTSHAGEN, U.Highly Luminescent ZnO Quantum Dots Made in a Nonthermal Plasma. **Adv Funct Mater,** v. 24, n. 14, p. 1988-1993, 2014.

GHOSH, M.; RAYCHAUDHURI, A. K. Optical Properties of Mg-Substituted ZnO Nanoparticles Obtained by Solution Growth. **IEEE Trans Nanotehcnol,** v. 10, n. 3, p. 555-559, 2011.

GUINIER, A.; FOURNET, G. **Small Angle Scattering of X-rays**. New-York: Wiley, 1955.

JIA, Z.; MISRA, R. D. K. Tunable ZnO quantum dots for bioimaging: synthesis and photoluminescence. **Mater Technol,** v. 28, n. 4, p. 221-227, 2013.

KLAINE, S. J.;ALVAREZ, P. J.; BATLEY, G. E.; FERNANDES, T. F.; HANDY, R. D.; LYON, D. Y.; MAHENDRA, S.; MCLAUGHLIN, M. J.; LEAD, J. R.Nanomaterials in the environment: Behavior, fate, bioavailability, and effects. **Environ Toxicol Chem,** v. 27, n. 9, p. 1825-1851, 2008.

KOLEVA, V.; STOILOVA, D. Infrared and Raman studies of the solids in the $Mg(CH_3COO)_2$–$Zn(CH_3COO)_2$–$H_2O$ system. **J Mol Struct,** v. 611, n. 1–3, p. 1-8, 2002.

LAYEK, A.;DE, S.; THORAT, R.; CHOWDHURY, A. Spectrally Resolved Photoluminescence Imaging of ZnO Nanocrystals at Single-Particle Levels. **J Phys Chem Lett,** v. 2, n. 11, p. 1241-1247, 2011.

LEWINSKI, N.; COLVIN, V.; DREZEK, R. Cytotoxicity of Nanoparticles. **Small,** v. 4, n. 1, p. 26-49, 2008.

LIN, Y.-J.; WU, P.-H.; TSAI, C.-L.;LIU, C.-J.;LIN, Z.-R.;CHANG, H.-C.;LEE, C.-T. Effects of Mg incorporation on the optical properties of ZnO prepared by the sol-gel method. **J Appl Phys,** v. 103, p. 113709, 2008.

LIU, D.-P.; LI, G. D.; SU, Y.; CHEN, J. S. Highly Luminescent ZnO Nanocrystals Stabilized by Ionic-Liquid Components. **Angew Chem Int Ed Engl,** v. 45, n. 44, p. 7370-7373, 2006.

MICHALET, X.; PINAUD, F. F.; BENTOLILA, L. A.; TSAY, J. M.; DOOSE, S.; LI, J. J.; SUNDARESAN, G.; WU, A. M.; GAMBHIR, S. S.; WEISS, S.Quantum Dots for Live Cells, in Vivo Imaging, and Diagnostics. **Science,** v. 307, n. 5709, p. 538-544, 2005.

MOUSSODIA, R.-O, BALAN, L., MERLIN, C.,MUSTIN, C., SCHNEIDER, R. Biocompatible and stable ZnO quantum dots generated by functionalization with siloxane-core PAMAM dendrons. **J Mater Chem**, v. 20, p. 1147-1155, 2010.

NORBERG, N. S.; KITTILSTVED, K. R.; AMONETTE, J. E.; KUKKADAPU, R. K.; SCHWARTZ, D. A.; GAMELIN, D. R. Synthesis of Colloidal Mn2+:ZnO Quantum Dots and High-TC Ferromagnetic Nanocrystalline Thin Films. **J Am Chem Soc,** v. 126, n. 30, p. 9387-9398, 2004.

PARK, J.-H.;VON MALTZAHN, G.; RUOSLAHTI, E.; BHATIA, S. N.; SAILOR, M. J.Micellar Hybrid Nanoparticles for Simultaneous Magnetofluorescent Imaging and Drug Delivery. **Angew Chem Int Ed Engl,** v. 47, n. 38, p. 7284-7288, 2008.

SCHWARTZ, D. A.;NORBERG, N. S.; NGUYEN, Q. P.; PARKER, J. M.; GAMELIN, D. R. Magnetic Quantum Dots: Synthesis, Spectroscopy, and Magnetism of Co2+- and Ni2+-Doped ZnO Nanocrystals. **J Am Chem Soc,** v. 125, n. 43, p. 13205-13218, 2003.

SU, Y.; HE, Y.; LU, H.; SAI, L.; LI, Q.; LI, W.; WANG, L.; SHEN, P.; HUANG, Q.; FAN, C. The cytotoxicity of cadmium based, aqueous phase – Synthesized, quantum dots and its modulation by surface coating. **Biomaterials,** v. 30, n. 1, p. 19-25, 2009.

TIAN, B.;AL-JAMAL, W. T.; AL-JAMAL, K. T.; KOSTARELOS, K. Doxorubicin-loaded lipid-quantum dot hybrids: Surface topography and release properties. **Int J Pharm,** v. 416, n. 2, p. 443-447, 2011.

VAN DIJKEN, A.;MEULENKAMP, E. A.;VANMAEKELBERGH, D.;MEIJERINK, A.The Kinetics of the Radiative and Nonradiative Processes in Nanocrystalline ZnO Particles upon Photoexcitation. **J Phys Chem B,** v. 104, n. 8, p. 1715-1723, 2000.

VIJAYALAKSHMI, K.; KARTHICK, K. Influence of Mg doping on the microstructure and PL emission of wurtzite ZnO synthesized by microwave processing. **J Mater Sci Mater Electron,** v. 24, n. 6, p. 2067-2071, 2013.

WANG, C.; GAO, X.; SU, X. In vitro and in vivo imaging with quantum dots. **Anal Bioanal Chem,** v. 397, n. 4, p. 1397-1415, 2010.

WEST, A. R. **Solid State Chemistry and Its Applications**. New York: John Wiley and Sons 1992.

XIE, J.; LEE, S.; CHEN, X. Nanoparticle-based theranostic agents. **Adv Drug Deliv Rev,** v. 62, n. 11, p. 1064-1079, 2010.

XIONG, H.-M.;SHCHUKIN, D. G.; MÖHWALD, H.; XU, Y.; XIA, Y. Y. Sonochemical Synthesis of Highly Luminescent Zinc Oxide Nanoparticles Doped with Magnesium(II). **Angewandte Chemie,** v. 121, n. 15, p. 2765-2769, 2009.

XIONG, H.-M. Photoluminescent ZnO nanoparticles modified by polymers. **J Mater Chem,** v. 20, n. 21, p. 4251-4262, 2010.

XIONG, H.-M. ZnO Nanoparticles Applied to Bioimaging and Drug Delivery. **Adv Mater**, v. 25, p. 5329–5335, 2013.

XU, X.;XU, C.;WANG, X.;LIN, Y.;DAI, J.;HU, J. Control mechanism behind broad fluorescence from violet to orange in ZnO quantum dots. **CrystEngComm,** v. 15, n. 5, p. 977-981, 2013.

YANG, Y.;JIN, Y.; HE, H.; WANG, Q.; TU, Y.; LU, H.; YE, Z.Dopant-Induced Shape Evolution of Colloidal Nanocrystals: The Case of Zinc Oxide. **J Am Chem Soc,** v. 132, n. 38, p. 13381-13394, 2010.

YOUSEFI, R.;SHEINI, F. J.; MUHAMAD,M. R.;MORED, M. A. Characterization and field emission properties of ZnMgO nanowires fabricated by thermal evaporation process. **Solid State Sciences,** v. 12, n. 7, p. 1088-1093, 2010.

YOUSEFI, R.; KAMALUDDIN, B. Fabrication and characterization of ZnO and ZnMgO nanostructures grown using a ZnO/ZnMgO compound as the source material. **Appl Surf Sci,** v. 256, n. 1, p. 329-334, 2009.

YOUSEFI, R.; ZAK, A. K.; JAMALI-SHEINI, F. Growth, X-ray peak broadening studies, and optical properties of Mg-doped ZnO nanoparticles. **Mater Sci Semicond Process,** v. 16, n. 3, p. 771-777, 2013.

ZHANG, L.;YIN, L.;WANG, C.;LUN, N.;QI, Y.;XIANG, D. Origin of Visible Photoluminescence of ZnO Quantum Dots: Defect-Dependent and Size-Dependent. **J Phys Chem CNanomater Interfaces,** v. 114, n. 21, p. 9651-9658, 2010.

## V.4. REFERENCES

ABED, N.; COUVREUR, P. Nanocarriers for antibiotics: A promising solution to treat intracellular bacterial infections. **Int J Antimicrob Agents**, v. 43, p. 485-496.

ADEREM, A.; UNDERHILL, D. M. MECHANISMS OF PHAGOCYTOSIS IN MACROPHAGES. **Annu Rev Immunol,** v. 17, n. 1, p. 593-623, 1999.

AL-JAMAL, W. T.; AL-JAMAL, K. T.; TIAN, B.; LACERDA, L.; BOMANS, P. H.; FREDERIK, P. M.; KOSTARELOS, K. Lipid−Quantum Dot Bilayer Vesicles Enhance Tumor Cell Uptake and Retention in Vitro and in Vivo. **ACS Nano,** v. 2, n. 3, p. 408-418, 2008.

DUBERTRET, B.;SKOURIDES, P.; NORRIS, D. J.; NOIREAUX, V.; BRIVANLOU, A. H.; LIBCHABER, A. In Vivo Imaging of Quantum Dots Encapsulated in Phospholipid Micelles. **Science,** v. 298, n. 5599, p. 1759-1762, 2002.

GARCÍA, I.;SÁNCHEZ-IGLESIAS, A.; HENRIKSEN-LACEY, M.; GRZELCZAK, M.; PENADÉS, S.; LIZ-MARZÁN, L. M. Glycans as Biofunctional Ligands for Gold Nanorods: Stability and Targeting in Protein-Rich Media. **J Am Chem Soc,** v. 137, n. 10, p. 3686-3692, 2015.

GOPALAKRISHNAN, G.;DANELON, C.; IZEWSKA, P.; PRUMMER, M.; BOLINGER, P. Y.; GEISSBÜHLER, I.; DEMURTAS, D.; DUBOCHET, J.; VOGEL, H.Multifunctional Lipid/Quantum Dot Hybrid Nanocontainers for Controlled Targeting of Live Cells. **Angew Chem Int Ed Engl,** v. 45, n. 33, p. 5478-5483, 2006.

HILLAIREAU, H.; COUVREUR, P. Nanocarriers' entry into the cell: relevance to drug delivery. **Cell Mol Life Sci,** v. 66, n. 17, p. 2873-2896, 2009.

JAULIN, N.;APPEL, M.; PASSIRANI, C.; BARRATT, G.; LABARRE, D. Reduction of the Uptake by a Macrophagic Cell Line of Nanoparticles Bearing Heparin or Dextran Covalently Bound to Poly(methyl methacrylate). **J Drug Target,** v. 8, n. 3, p. 165-172, 2000.

JOHNSSON, M.; HANSSON, P.; EDWARDS, K. Spherical Micelles and Other Self-Assembled Structures in Dilute Aqueous Mixtures of Poly(Ethylene Glycol) Lipids. **J Phys Chem B,** v. 105, n. 35, p. 8420-8430, 2001.

LEPELTIER, E.; BOURGAUX, C.; COUVREUR, P. Nanoprecipitation and the "Ouzo

effect": Application to drug delivery devices. **Adv Drug Deliv Rev,**v. 71, p. 86-97, 2014.

SALEM, I. I.; FLASHER, D. L.; DÜZGÜNEŞ, N. Liposome-Encapsulated Antibiotics1. In: (Ed.). **Methods Enzymol**, 2005. v. 391, p.261-291.

SCHROEDER, J. E.;SHWEKY, I.; SHMEEDA, H.; BANIN, U.; GABIZON, A.Folate-mediated tumor cell uptake of quantum dots entrapped in lipid nanoparticles. **J Control Release,** v. 124, n. 1–2, p. 28-34, 2007.

WI, H. S.;KIM, S. J.; LEE, K.; KIM, S. M.; YANG, H. S.; PAK, H. K. Incorporation of quantum dots into the lipid bilayer of giant unilamellar vesicles and its stability. **Colloids Surf B Biointerfaces,** v. 97, n. 0, p. 37-42, 2012.

# CHAPTER VI
# Final conclusions and perspectives

# Chapter VI – Final conclusions and perspectives

## VI.1. Final conclusions

The aim of this thesis was to explore ZnO based QDs as bioimaging agents due to their promising photoluminescent properties, when synthesized via sol-gel route, and low toxicity compared to the usual QDs, which contain heavy metals such as Cd, Pb, etc.

In a first step, attempts were made to improve the photoluminescence properties of ZnO QDs by synthesizing ZnO/ZnS core-shell QDs and doping ZnO QDs with $Mg^{2+}$ ions. Hereafter, QD surface modification was achieved for later incorporation in lipid based nanocarriers. Finally, the study of the structure, stability, photoluminescence properties and cell internalization of lipid nanocarriers loaded with QDs was carried out.

We could monitor the reactions tentatively used for obtaining ZnO/ZnS core-shell QDs and characterize the final products. We could observe that a small amount of TAA in the reaction medium was not sufficient to produce ZnS; an intermediate amount of TAA led to the formation of both species (ZnO and ZnS); and higher quantities of TAA gave mainly rise to ZnS nanoparticles. Figure VI.1 shows schematically the final products starting from either ZnAc precursor or ZnO colloidal suspensions mixed with three different TAA concentrations. The samples obtained in each reaction could be characterized by UV-vis, XRD and XAS techniques; however, it is noteworthy that only XAS allowed identifying core-shell structure when the reaction proceeded in ZnO colloidal suspension mixed with TAA 5 mM (Route1).

**Figure VI.1.**Schematical final products obtained in the reactions starting from ZnO colloidal suspensions (Route 1) and ZnAc precursor (Route 2) using three TAA concentrations (1.5, 5 and 50mM).

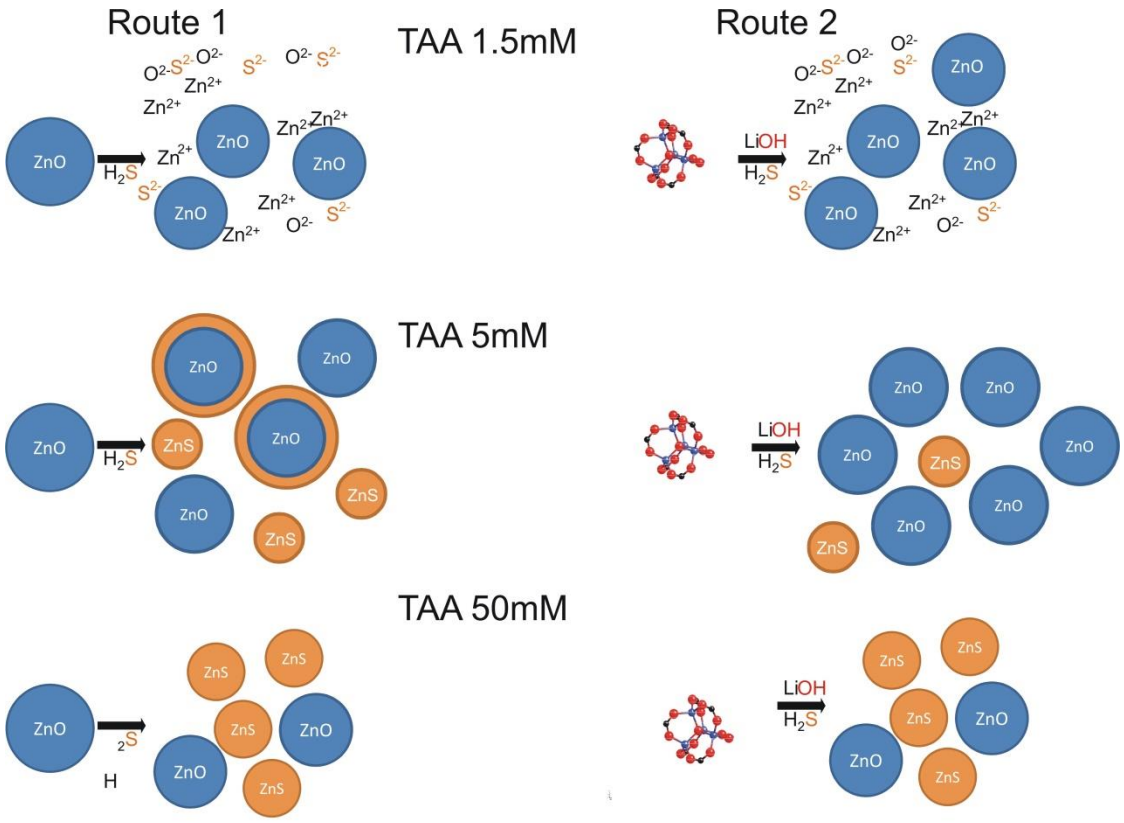


ZnO/ZnS QDs showed a rather weak photoluminescence in the visible range, compared to ZnO QDs, without displaying a significantly increased emission in the UV range. Therefore, doping of Zno QDs with Mg ions was performed in an attempt to optimize their luminescence.

Mg-doped ZnO QDs were synthesized,preserving the wurtzite lattice of ZnO. The higher was the amount of dopant incorporated into ZnO structure, smaller was the size of nanoparticles. Mg ions incorporated into ZnO QDs strongly changed their growth, preventing the formation of fractal aggregates. We could increase the QY of ZnO QDs six times by using 20 mol% (nominal concentration) of $Mg^{2+}$ ions in the reaction medium. The modification of their surface was also requiredto incorporate them into lipid-based nanocarriers. The ZnO and $Zn_{0.8}Mg_{0.2}O$ QDs could be successfully capped by oleic acid (OA), forming stable colloidal dispersions in chloroform and toluene and keeping strong visible luminescence. Figure VI.2 presents schematically the structures of ZnO and $Zn_{0.8}Mg_{0.2}O$ QDs with and without OA

coating, their photographs and respective QY. This part of the work has already been published in the European Journal of Nanomedicine, 7(2): 109–120, 2015 (Annexe).

**Figure VI.2.**Schematical structures of ZnO and $Zn_{0.8}Mg_{0.2}O$ QDs with and without OA capping, their photographs and respective QY.

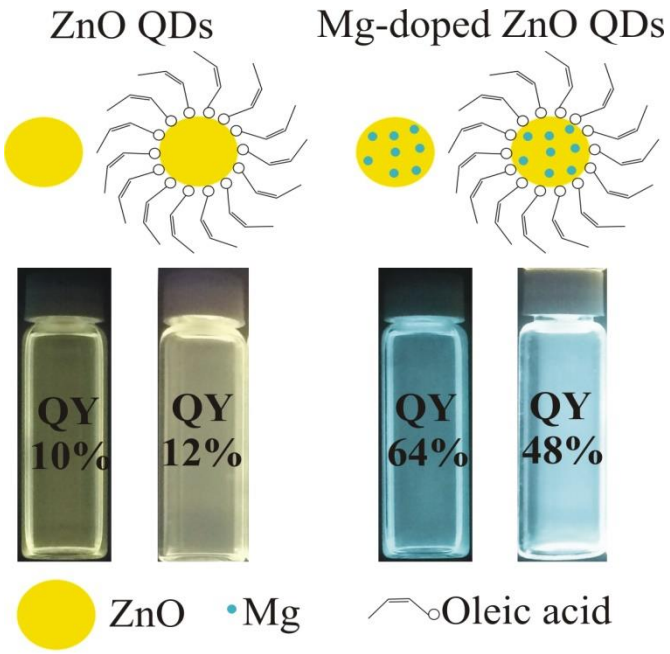


Finally, we have tried to incorporate highly luminescent $Zn_{0.8}Mg_{0.2}O$ and OA-$Zn_{0.8}Mg_{0.2}O$ QDs into lipid-based nanocarriers.

Figure VI.3 shows examples of photographs of liposomes, DSPE-Peg based formulations and SLNs, loaded with QDs. As observed in this figure, liposomes presented lower luminescence compared to the DSPE-Peg formulation and SLN. SLNs were fairly stable in biological media, as shown by the absence of large aggregates. However, further investigations are needed to optimize the preparation and photoluminescence properties of the different nanocarriersfor bioimaging applications.

**Figure VI.3.**Photographs of QDs loaded liposomes, a DSPE-Peg based formulation and an example of SLN (from left to right, respectively) under UV lamp.

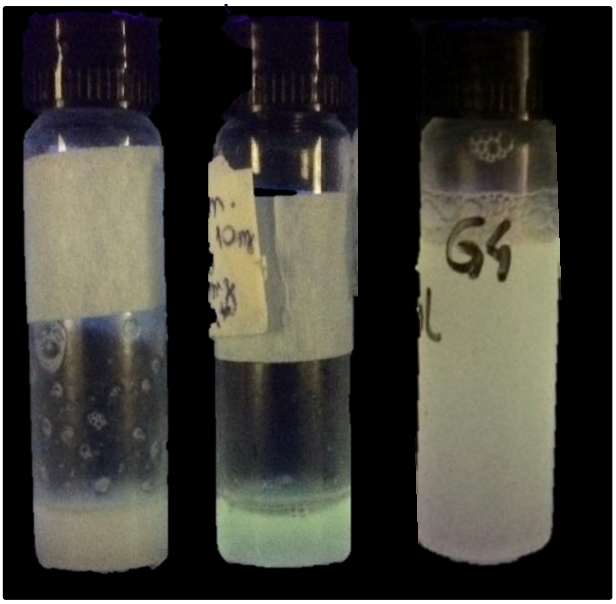

## VI.2. Perspectives

ZnO/ZnS nanoparticles surface could be characterized by XPS, Zeta potential and isoeletric potential to confirm the modification of their surface by the ZnS shell deposition around the ZnO core.

Doping with $Mg^{2+}$ ions widened the band gap of ZnO QDs and enhanced their visible luminescence. While studying Mg-doped ZnO QDs we could observe that $Mg^{2+}$ ions interfere directly with the growth of the nanoparticles, inducing disorder in the ZnO lattice, decreasing the final size of the QDs and hindering their aggregation.However, we could not determine their location into ZnO QDs (in the core and/or at the surface). EXAFS and XANES spectra could be recorded at the Mg edge to identify the environment of Mg ions (nature and number of neighbors, distance between them). Indeed, no significant differences could be evidenced at the Zn edge between ZnO QDs and Mg-doped Zno QDs. First experiments have been performed at LUCIA beamline at SOLEIL Synchrotron source. Work is in progress.

Regarding DPPC-based formulations which preserve the DPPC bilayer structure, atomic force microscopy (AFM) could be used to investigate the homogeneity of the repartition of QDs in the bilayers and the potential presence of QD aggregates. Further investigations are needed to better control the size and size distribution of the different nanocarriers, improve their luminescence and characterize their structure.

For cell internalization studies, the limitations due to the cell auto-fluorescence phenomena might be overcome if ZnO QDs were excited at the optimal excitation wavelength with high intensity beam and short exposure time.Appropriate setups are available at the DISCO beamline at SOLEIL. Besides, the luminescent nanoparticle formulation, concentration and time of incubation with cells should be optimized.

# ANNEXES

DE GRUYTER Eur. J. Nanomed. 2015; 7(2): 109–120

Eloísa Berbel Manaia, Renata Cristina Kiatkoski Kaminski, Bruno Leonardo Caetano, Valérie Briois, Leila Aparecida Chiavacci and Claudie Bourgaux*

# Surface modified Mg-doped ZnO QDs for biological imaging

**Abstract:** Nanocrystals of ZnO are currently attracting great interest as potential labels for biological applications, such as theranostic devices, due to their luminescent properties and low toxicity in vivo. It has been reported that doping with $Mg^{2+}$ ions could enhance the luminescence of ZnO quantum dots (QDs). In the present study Mg-doped ZnO QDs were synthesized by a hydrolysis and condensation reaction. Surface modification of the QDs was performed using oleic acid (OA) to hinder their aggregation and to provide them colloidal stability in non-polar environments. $Mg^{2+}$ ions could be incorporated into the ZnO wurtzite lattice owing to the very close values of the $Mg^{2+}$ and $Zn^{2+}$ ion radii. However, the dopant ions strongly influenced the growth and final size of ZnO nanocrystals, as evidenced by time-resolved synchrotron SAXS measurements. The presence of Mg prevented the aggregation of the primary nanoparticles. Doping with $Mg^{2+}$ ions widened the band gap of ZnO QDs and enhanced their visible luminescence. With increasing proportion of $Mg^{2+}$ ions, both the absorption and emission spectra experienced a blue shift. The luminescence went through a maximum for a 20 mol% nominal concentration of $Mg^{2+}$ ions in the reaction medium. The quantum yield (QY) of 20 mol% Mg-doped ZnO colloidal suspension (64%) was about 6 times higher than that of the ZnO suspension (10%). Mg-doped ZnO QDs capped by OA formed stable colloidal dispersions in chloroforme, with strong visible fluorescence (QY=38%), promising for biological imaging.

**Keywords:** biological imaging; Mg-doped ZnO quantum dots; SAXS; sol-gel process.

DOI 10.1515/ejnm-2014-0047
Received November 16, 2014; accepted March 12, 2015

***Corresponding author: Claudie Bourgaux,** University Paris-Sud, Institut Galien, CNRS, UMR 8612, LabEX LERMIT, F-92296 Châtenay-Malabry, France, Phone: +33 1 46 83 58 68, Fax: +33 1 46 83 53 12, E-mail: claudie.bourgaux@u-psud.fr

**Eloísa Berbel Manaia:** Faculty of Pharmaceutical Sciences of São Paulo State University, UNESP, Araraquara-Jaú Interstate Highway, Km 1, Araraquara, SP, Brazil; University Paris-Sud, Institut Galien, CNRS, UMR 8612, LabEX LERMIT, F-92296 Châtenay-Malabry, France

**Renata Cristina Kiatkoski Kaminski:** Sergipe Federal University, Campus Itabaiana, Av. Vereador Olimpio Grande, s/n, Itabaiana, SE, Brazil

**Bruno Leonardo Caetano:** Chemistry Institute of São Paulo State University, UNESP, Prof. Francisco Degni Street, 55, Araraquara, SP, Brazil

**Valérie Briois:** Synchrotron SOLEIL, L'Orme des Merisiers, BP48, Saint Aubin, 91192 Gif-sur Yvette, France

**Leila Aparecida Chiavacci:** Faculty of Pharmaceutical Sciences of São Paulo State University, UNESP, Araraquara-Jaú Interstate Highway, Km 1, Araraquara, SP, Brazil

## Introduction

At the nanoscale, the optoelectronic properties of semiconductor crystals depend on their size. For crystals smaller than twice the Bohr exciton radius (the so-called quantum dots, QDs), the semi-conductor band gap widens as the nanocrystal size decreases, owing to quantum confinement effects. Consequently, the radiative recombination of an electron from the conduction band with a hole from the valence band leads to the emission of a photon whose wavelength can be tuned by changing the nanocrystal size. The creation of an electron-hole pair (or exciton) is induced by the absorption of a photon with energy above that of the band gap, resulting in a broad absorption spectrum. Both the absorption and emission spectra of QDs experience a blue shift with QD decreasing size (1).

Usual QDs are made of CdSe, CdTe, InAs and InP. Depending on their composition and size, their emission ranges from near UV to near IR. They need appropriate surface modification, such as coating with amphiphilic molecules, to be dispersible in an aqueous solution. When functionalized with ligands such as antibodies or peptides, QDs can be used to label different types of cellular targets or detect biomarkers (2, 3). Recently, nanoparticles containing QDs have been investigated as theranostic devices for simultaneous imaging and drug delivery (4). For instance, doxorubicine has been loaded, along with QDs, into micelles, aptamers, and liposomes (5–7).

However, the potential cytotoxicity of first generation QDs is a major concern for biological applications (8–11). In this context, luminescent nanoparticles of ZnO are currently attracting great interest as potential labels for bio-imaging because of their biodegradability and very low toxicity in vivo, although ZnO nanoparticles are able to release $Zn^{2+}$ ions and produce destructive reactive oxygen species (ROS), as shown by cytotoxicity tests in vitro (12–14). ZnO is an n-type semi-conductor with a wide band gap of 3.37 eV at room temperature and a Bohr exciton radius of ~2.34 nm. The typical excitonic emission, arising from recombination of photo-generated electrons with holes in the valence band or in traps near the valence band, is thus observed in the UV range. Remarkably, the photoluminescence spectrum of ZnO nanocrystals also displays a broad visible emission, more suitable for biological imaging, which has been ascribed to point defects such as O and Zn vacancies or interstitials and related to surface oxygen-containing moieties, such as OH groups (15). However, the understanding of the exact mechanism for visible emission is still lacking.

Because of the role of defects and surface chemistry, the synthesis technique is expected to strongly influence the luminescence of ZnO. In general, the visible emission of thin films or particles synthesized at high temperature or annealed is very weak whereas nanoparticles prepared by the sol-gel route exhibit stronger defect-induced visible luminescence. A typical sol-gel route is the hydrolysis and condensation of a precursor in ethanolic solution (Zn salt solution) catalyzed by a base (16). However, the obtained ZnO QDs display a low quantum yield and are unstable in water and in non-polar solvents. Surface modification is further required to prevent growth and aggregation of QDs and to ensure their colloidal stability in different environments (17). Obtaining ZnO QDs with high quantum yield while preserving their visible luminescence upon surface modification remain a challenge because of the sensitivity of photoluminescence to subtle changes of synthesis parameters and environment.

It has been reported that doping with $Mg^{2+}$ ions can enhance the luminescence of ZnO. Most of previous researches have focused on Mg-doped ZnO thin films and particles annealed at high temperature, with high UV emission but weak visible luminescence (18–22).

In the present study, we report the design of ZnO-based QDs with strong visible luminescence, promising for labeling of lipidic nanoparticles which could be used as theranostic devices. Specifically, we have shown that (i) Mg-doped ZnO QDs prepared using the sol-gel method exhibited enhanced visible luminescence, (ii) the maximum quantum yield was obtained for Mg precursor concentration of 20 mol%, (iii) Mg-doped ZnO QDs capped by oleic acid formed stable colloidal suspensions in toluene and chloroform, while preserving their photoluminescence.

Mg-doped ZnO QDs were characterized by elemental analysis, transmission electronic microscopy, small- and wide-angle X-ray scattering, Raman spectroscopy, UV-Vis absorption and photoluminescence emission. The aim was to establish a relationship between the composition and structure of the QDs and their luminescent properties.

## Materials and methods

### Materials

Zinc acetate dihydrate, $ZnAc_2{\cdot}2H_2O$ (Alfa Aesar), lithium hydroxide monohydrated, $LiOH{\cdot}H_2O$ (Alfa Aesar), magnesium acetate tetrahydrate, $Mg(Ac)_2{\cdot}4\ H_2O$ (Alfa Aesar), oleic acid (Alfa Aesar), ethanol (VWR, BDH, Prolabo), chloroform (VWR, BDH, Prolabo) and heptane (Carlo Erba Reagents), were used as received, without further purification. Zinc oxide powder (Alfa Aesar) was used as standard.

### Synthesis

**ZnO QDs:** ZnO colloidal suspensions were synthesized by hydrolysis and condensation at 60°C of a precursor solution ($Zn_4OAc_6$ ethanolic solution) upon mixing with a LiOH ethanolic solution, following the sol-gel route proposed by Spanhel and Anderson (23).

The $Zn_4OAc_6$ tetrameric precursor was first prepared by refluxing an absolute ethanol solution with 0.05 M $ZnAc_2{\cdot}2H_2O$ concentration for ~2 h at 80°C. The thus-obtained transparent precursor solution was stored at ~4°C. Meanwhile, $LiOH{\cdot}H_2O$ absolute ethanol solution (0.5 M) was prepared by ultrasonic mixing. Hydrolysis and condensation reactions were carried out in a flask containing the precursor solution thermostated at 60°C. LiOH solution was dropped into the precursor solution and the reaction medium was then continuously stirred for 30 min. Afterward, the ZnO colloidal suspension was cooled and stored at ~4°C to prevent any further growth process. The nominal molar ratio [OH]/[Zn] was 1.4.

**Mg-ZnO QDs:** Mg doping was achieved by adding a $Mg(Ac)_2$ ethanol solution to the Zn precursor solution, keeping the total molar concentration [Zn+Mg] constant. The [LiOH]/[Zn+Mg] molar ratio was also kept constant. The reaction conditions were similar to those described above for preparing undoped nanoparticles. The Mg precursor concentration was increased from 2.5 to 20 mol%. Samples are referred to using nominal $Mg^{2+}$ mole fraction in the initial reaction mixture (e.g. 20% Mg-ZnO).

**OA-ZnO QDs:** ZnO QDs capped by oleic acid (OA) were obtained by adding oleic acid to the ZnO QDs suspension (13 mM, 18.8 mM, 25 mM or 36.7 mM OA concentration) under vigorous stirring during 30 min at 60°C. The resulting turbid solutions were stored at 8°C overnight

and then centrifuged (10 min at 10,000 rpm, 13000 *g*). The supernatant was removed and the OA-ZnO QDs were washed with ethanol, in which they could not be dispersed, in order to remove the unreacted OA. Afterward, the washed OA-ZnO QDs were dried at room temperature under vacuum and put in suspension into chloroform or toluene.

**OA-Mg-ZnO QDs:** The surface modification of the 20% Mg-ZnO QDs, which showed optimal photoluminescence properties, was achieved in the same way.

**Powder obtention:** Doped or undoped ZnO QDs could be recovered from the ethanolic suspensions thanks to an extraction procedure using heptane. The as-synthesized colloidal suspensions were mixed with a "non-solvent" heptane (2:4) (1:4) to induce the precipitation of the QDs, and then centrifuged at 20°C for 10 min (10,000 rpm, 13000 *g*). The supernatant was discarded and the powder was dried under vacuum at room temperature. The dried powder was used for X-ray powder diffraction characterization, Mg quantification and Raman spectroscopy analyses.

### Characterization

**Inductively coupled plasma mass spectrometry (ICP-MS):** $Mg^{2+}$ concentrations in doped QDs were determined using inductively coupled plasma mass spectrometry at the Institut des Sciences Analytiques, Villeurbanne.

**High resolution transmission electron microscopy (HRTEM):** HRTEM investigations were performed with a JEOL JEM-2011 UHR scanning electron microscope operating at 200 keV, at the "Service of electronic microscopy" at the University Pierre and Marie Curie, Paris, France. A drop of the dilute colloidal suspension of QDs was deposited on a copper grid. Image analysis was carried out with the ImageJ software.

**X-ray powder diffraction (XRD):** XRD analysis of nanoparticles was performed on a Bruker D2 PHASER diffractometer, using the Cu Kα radiation, $\lambda$=1.5418 Å, selected by a curved graphite monochromator and a fixed divergence slit of 1/8° in a Bragg-Brentano configuration. The diffraction intensity data were measured in the 2θ range 5–70° by the step counting method (0.1° step and 3 s counting time).

**Small-angle X-ray scattering (SAXS):** SAXS experiments were performed on the SWING beamline, operated at 10.5 keV, at the SOLEIL synchrotron source (Saint Aubin, France).

For two compositions, pure ZnO and 20 % Mg-ZnO, the nucleation and growth of nanoparticles have been followed in situ, using a home-made stopped-flow device. The freshly prepared precursor solution and the ethanolic LiOH solution, contained in two syringes, were simultaneously pushed by syringe pumps into two tubes, rapidly mixed at the Y-junction of these tubes and introduced into the thermostated X-ray capillary. The temperature of the sample holder was set to 60°C. Time-resolved SAXS patterns could be recorded from the first seconds of the reaction. The acquisition time of each curve was 200 ms. The dead time between two acquisitions was adjusted to take into account the evolution of the nanoparticle growth rate during synthesis.

SAXS patterns were collected by a two-dimensional CCD detector with a sample-to-detector distance of 1727 mm. The scattered intensity was reported as a function of the scattering vector $q=4\pi \sin\theta/\lambda$, where $2\theta$ is the scattering angle and $\lambda$ the wavelength of the incident beam. The calibration of the $q$ range (0.0062–0.64 $Å^{-1}$) was carried out with silver behenate.

Intensity values were normalized to account for beam intensity, acquisition time and sample transmission. Each scattering pattern was then integrated circularly to yield the intensity as a function of $q$. The scattered intensity from a capillary filled with ethanol was subtracted from the sample scattering curves. The analysis of the SAXS data was carried out using the software package SASFIT (25).

**Raman spectroscopy:** The Raman spectra were collected in the backscattering configuration at room temperature with a commercial Kaiser Optical Systems RXN1 Raman spectrometer equipped with a near-IR laser diode working at 785 nm, operating with a power output of 50 mW. All the samples, apart from liquid oleic acid, were dried powders.

**Spectroscopy UV:** The absorption spectra were measured using a Cary Win 4000 UV-Vis spectrophotometer with a cuvette of 1 mm optical path. The spectra of the QDs suspensions were recorded between 250 and 450 nm, with a wavelength step of 1 nm, and an average counting time of 0.2 s per point. The UV-vis spectra were corrected from the absorption spectrum of ethanol.

**Photoluminescence spectroscopy (PL):** The emission (PL) and excitation (PLE) photoluminescence spectra were recorded on a Luminescence spectrometer LS50B (Perkin-Elmer) at room temperature with a Xe lamp (20 kW) as the excitation source. For PL measurements, each sample was excited at the optimal wavelength, defined by the PLE spectrum (Table 1).

The quantum yield (QY) determines the efficiency of the conversion of absorbed photons into emitted ones. Usually, the relative QY of the studied sample is compared with that of a reference fluorophore. In this work, a solution of Rhodamine 6G in ethanol (QY=95%), often used as reference for green emission, was selected as the standard (26). According to the method described by Crosby and Demas (27), the QY is given by the following formula:

$$QY_x = QY_r [A_r(\lambda_r)/A_x(\lambda_x)](n_x^2/n_r^2)(D_x/D_r)$$

where $A$ is the absorbance at the excitation wavelength ($\lambda$), $n$ the refractive index of the solvent used and $D$ the integrated fluorescence intensity (the area under the corrected emission curve). The subscripts r and x refer to the reference and sample solutions, respectively. To minimize the errors, the same excitation wavelength was chosen to measure the PL spectra of the Rhodamine 6G and QD solutions and the two solutions had the same absorbance at this wavelength ($A$=0.05).

## Results

Mg-doped ZnO QDs were synthesized by the hydrolysis and condensation reaction described above. Surface modification of the QDs was performed using oleic acid (OA) to hinder their aggregation and to provide them colloidal stability in different environments. Different quantities of

**Table 1:** Amount of Mg incorporated into ZnO QDs obtained by ICP, crystallite size deduced from X-ray diffraction peaks using the Debye-Scherrer relation, bandgap measured using UV/Vis absorption, wavelength of the PLE peak maximum, wavelength of the PL emission peak maximum, quantum yield of each sample.

| Initial Mg mole fraction | Mg incorporated into ZnO, % | Crystallite size, nm | Bandgap, eV | $\lambda_{ex}$, nm | $\lambda_{em}$, nm | QY, % |
|---|---|---|---|---|---|---|
| 0 | | 3.3 | 3.37 | 365 | 520 | 10.2 |
| 2.5 | 0.41 | 2.7 | 3.42 | 363 | 520 | 5.0 |
| 5 | 0.72 | 2.3 | 3.52 | 358 | 512 | 16.7 |
| 10 | 1.98 | 2.2 | 3.60 | 350 | 476 | 27.8 |
| 20 | 2.94 | 2.0 | 3.71 | 342 | 470 | 64.8 |

OA were added to the QD suspensions. In all cases the QDs capped by OA formed stable colloidal dispersions in chloroform or toluene.

Preliminary measurements having shown that the visible luminescence of Mg-ZnO QDs went through a maximum for a 20 mol% nominal concentration of $Mg^{2+}$ ions in the reaction medium, our investigations focused on the structure and properties of QDs obtained with $Mg^{2+}$ concentration increasing up to 20%.

Actual atomic concentrations of Mg in doped QDs, determined using ICP-MS, are reported in Table 1. These data evidence a low incorporation of $Mg^{2+}$ ions into ZnO QDs. The $Mg^{2+}$ concentration varied from 0.41 to 2.94%.

Figure 1A shows powder wide-angle X-ray diffraction patterns, recorded between $2\theta=5°$ and 70°, of ZnO reference, ZnO QDs and Mg-ZnO QDs. They display peaks characteristic of the ZnO hexagonal wurtzite structure. No peak characteristic of the MgO rock salt phase (e.g., at 42.5°) is detected whatever the concentration of $Mg^{2+}$ ions.

The broadening of the peaks of Mg-ZnO QDs could result from a decrease in crystallinity and/or crystal size, promoted by the presence of Mg. Assuming that this broadening is mainly due to size effects, the average size of nanocrystals could be estimated using the Debye-Scherrer relation (28) applied to the (100) reflection:

$$D=\frac{\kappa\lambda}{\beta\cos\theta}$$

where $D$ is the crystal size; $k$ is a constant (shape factor, 0.89 for spherical nanoparticles), $\lambda$ is the X-ray wavelength, $\beta$ is the full width at half maximum (FWHM) of the diffraction peak and $2\theta$ is the diffraction angle. The size of the nanocrystals decreased from 3.3 nm for ZnO to 2.0 nm for 20% Mg-ZnO. Figure 1B shows a zoom of the (100) diffraction peak between $2\theta=30°$ and $2\theta=34°$. $Mg^{2+}$ ions shift the (100) peak to slightly higher angles, suggesting a weak decrease of the lattice parameters. This small change, whose extent depends on the Mg

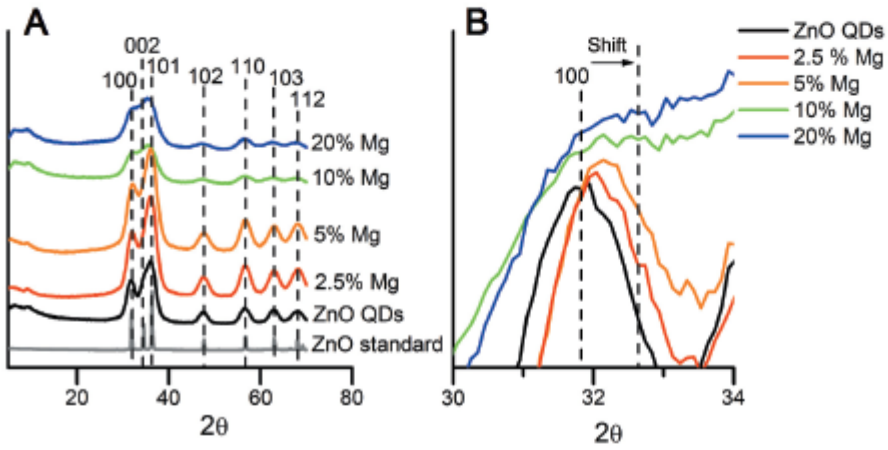


**Figure 1:** (A) XRD profiles of ZnO standard and 0, 2.5, 5, 10 and 20% of Mg-ZnO QDs, showing the presence of the hexagonal wurtzite phase (B) zoom of the (100) peak in the 30°–34° $2\theta$ range.

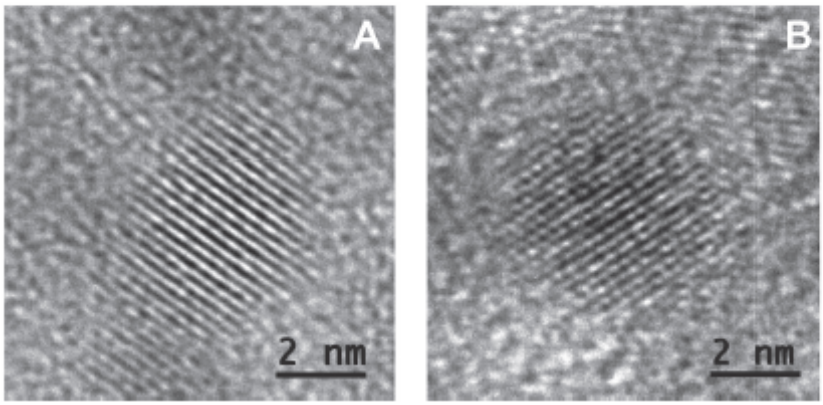


**Figure 2:** HRTEM images of undoped ZnO QDs (A) and 20% Mg-ZnO QDs (B).

concentration, is expected to reflect the substitution of some $Zn^{2+}$ ions by $Mg^{2+}$ ions in the crystalline lattice, as the $Mg^{2+}$ ions have a slightly smaller ionic radius (0.57 Å for $Mg^{2+}$ ions compared to 0.60 Å for $Zn^{2+}$ ions). At high Mg concentrations the peak shifts are obscured by the large width of the peaks.

The size and morphology of ZnO and 20% Mg-ZnO nanoparticles were also studied using HRTEM (Figure 2). HRTEM images show nanocrystals with approximately spherical shapes and average diameters of about 4 nm for ZnO QDs. The average size of Mg-ZnO QDs, whose structure appears less ordered, is slightly smaller. Overall, these data are in agreement with XRD data.

The influence of Mg on the growth of nanoparticles was further evidenced by time-resolved SAXS patterns, recorded from the beginning of the reaction. Figures 3A and 4A present three-dimensional stacked log-log plots of the SAXS curves as a function of time, corresponding to the formation of ZnO and 20% Mg-ZnO QDs, respectively. Selected curves of ZnO and 20% Mg-ZnO QDs formation are shown in Figures 3B and 4B, respectively. The two systems exhibit clearly different time evolution.

At the beginning of the reaction, ZnO curves display a plateau at low q-range (Guinier region), indicative of the scattering of non-interacting particles. In the Guinier region, the scattered intensity can be approximated by $I(q)=I(0)\exp(-Rg^2q^2/3)$ where $Rg$ is the radius of gyration (Guinier radius) of the particles (29). The Guinier plateau progressively shifts to lower $q$-values, reflecting the increase in the nanoparticle size with time. The curves display an oscillation at high $q$-values, which can arise from the form factor of spherical particles. The SAXS profiles could be fitted by the form factor of homogeneous spheres with Gaussian radius distribution. The radii of gyration $Rg$ are consistent with the mean radii of the nanoparticles $R$, as deduced from the fits [for a sphere $Rg$ is defined as $Rg=(3/5)^{1/2}R$] (Figure 5A). The size of the nanoparticles increased steeply during the first minutes of the reaction, up to 3 nm after 3 min. After about 15 min the size of the primary particles, which has reached 4 nm, no longer evolved.

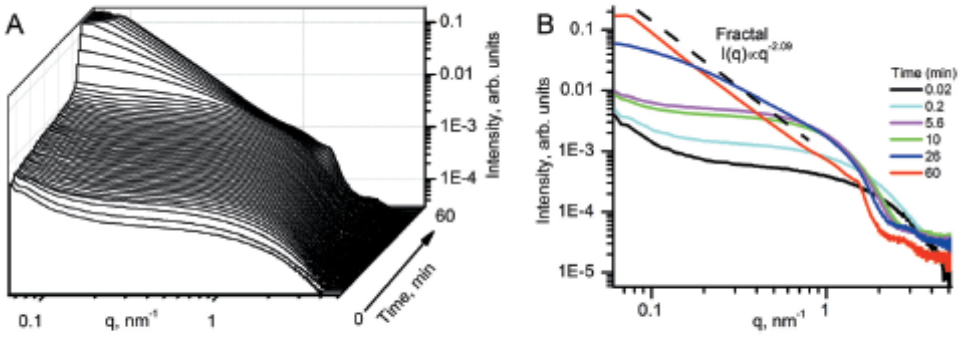


**Figure 3:** Three-dimensional stacked log-log plots of the SAXS curves as a function of time recorded in situ during the formation of ZnO QDs (A) and selected in situ SAXS profiles measured at the indicated reaction time (min) (B).

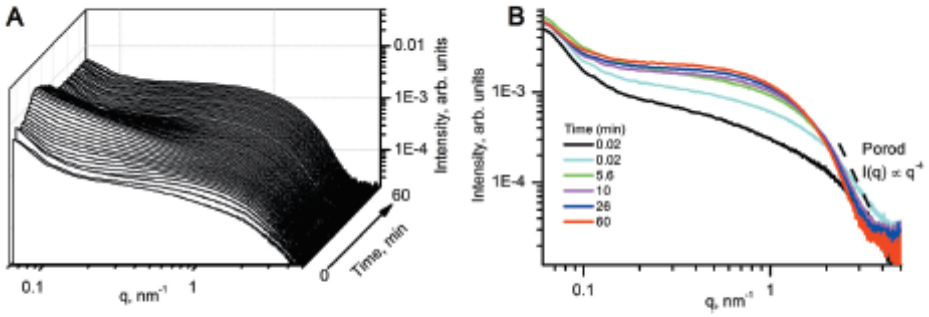


**Figure 4:** Three-dimensional stacked log-log plots of the SAXS curves as a function of time recorded in situ during the formation of 20% Mg-doped ZnO QDs (A) and selected in situ SAXS profiles measured at the indicated reaction time (min) (B).

At the end of the reaction, after about 50 min, the intensity scattered at low $q$-values strongly increases and the Guinier plateau disappears. In the low $q$ region, a linear decay of log$I$ is observed in the log$I$ vs. log$q$ plot: $I(q) \propto q^{-\alpha}$ (30) with $\alpha$=2.09. This behaviour evidences the formation of fractal aggregates with fractal dimension α, defined as the exponent that relates the mass M of an object to a characteristic dimension R: $M \propto R^{\alpha}$. The $\alpha$=2.09 fractal dimension is characteristic of structures formed by reaction-limited cluster-cluster aggregation (RLCCA). The aggregation rate is limited by the time needed to overcome the repulsive barrier between two clusters. Compared to the diffusion-limited cluster-cluster aggregation (DLCCA), the RLCCA mechanism corresponds to slower colloid aggregation, yielding more compact clusters due to the lower sticking probability (31).

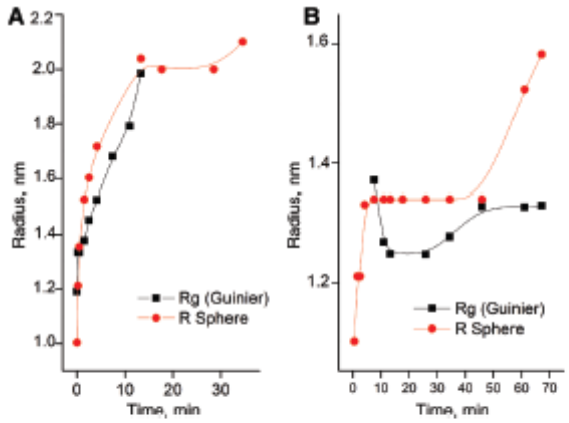


**Figure 5:** Comparison of the time evolution of the radius of gyration ($Rg$), determined in the Guinier region, and the radius ($R$), deduced from the fit of curves by the form factor of spheres, of nanoparticles: (A) ZnO QDs and (B) 20% Mg-ZnO QDs.

This linear decrease in log$I$ as a function of log$q$ is observed between $q$-values corresponding to the primary particle size and the fractal aggregate size, respectively. As shown by the curve oscillation in the high $q$ range, the mean radius of the primary particles remains constant, at about 2 nm, until the end of the reaction. Consequently, the formation of ZnO QDs involves two main steps: the nucleation and growth, up to a size of ~4 nm, of elementary nanoparticles during the ten first min of the reaction, followed by the formation of fractal aggregates with fractal dimension $\alpha$=2.09.

The structures giving rise to the first Mg-ZnO SAXS profiles collected during the synthesis of Mg-ZnO QDs could not be identified. After about 5 min, the SAXS curves could also be fitted by the form factor of homogeneous spheres with Gaussian radius distribution. The growth of nanoparticles is rapidly stopped after the nucleation step. Nanoparticles remain smaller than ZnO ones. A further small increase in size is observed at the end of the reaction. The intensity $I(0)$, proportional to the number of nanoparticles in the medium, increases continuously during the first 60 min of the reaction. Of note, unlike ZnO nanoparticles, Mg-ZnO QDs do not form fractal aggregates with time, suggesting that the nanoparticles have different surface properties.

Raman scattering carried out on QDs allows obtaining information on the surface species and on the modifications of the optical phonon spectrum, as compared to ZnO bulk crystal values (Figure 6A and B).

The spectrum of ZnO standard shows a prominent peak at 439 $cm^{-1}$ and weak peaks at 332 $cm^{-1}$, 380 $cm^{-1}$, 410 $cm^{-1}$, 581 $cm^{-1}$ and 666 $cm^{-1}$, in agreement with previous studies (32). The peak at 439 $cm^{-1}$ is characteristic of the wurtzite lattice; the sharp line shape is indicative of high crystalline order. This peak becomes less intense in ZnO QDs while the intensity of the 410 $cm^{-1}$ band increases, appearing as a shoulder of the peak at 439 $cm^{-1}$.

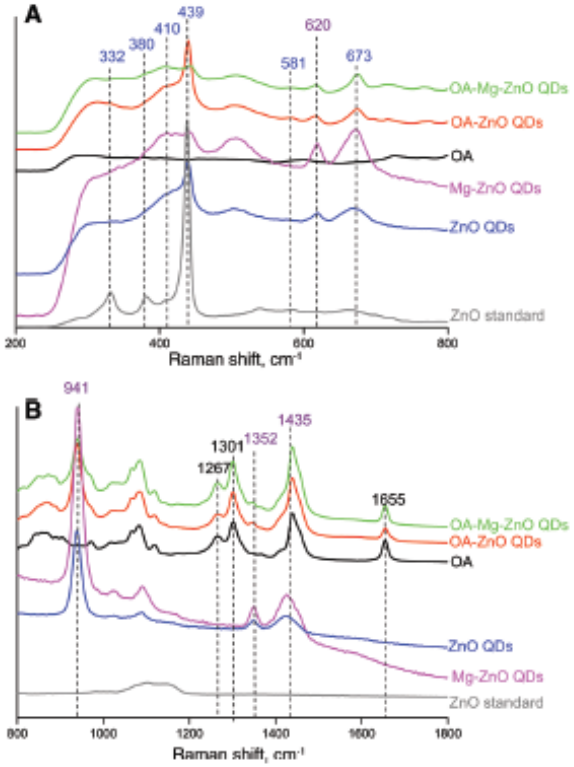


**Figure 6:** Raman spectra of ZnO standard, ZnO QDs, Mg-ZnO QDs, OA, OA-ZnO QDs and OA-Mg ZnO QDs with indications of the principal vibrations (A) from 200 to 800 $cm^{-1}$ and (B) from 800 to 1800 $cm^{-1}$.

More importantly, in Mg-ZnO QDs the weak 439 $cm^{-1}$ peak is involved in a broad band, reflecting the diminution of crystallinity induced by Mg incorporation.

The presence of oleic acid (OA) attached on the surface of QDs is unambiguously evidenced by the intense and well resolved peaks at 1265 $cm^{-1}$, 1301 $cm^{-1}$ and 1655 $cm^{-1}$ which cannot overlap with peaks arising from other species. These peaks correspond to δ(=CH) deformations, $\delta(CH_2)_n$ deformations and ν(C=C) stretching vibrations of unsaturated fatty acids, respectively (33). Other peaks assigned to OA (34) are listed in Table 2.

Beside peaks originating from the optical phonon spectrum of QDs and OA molecules capping their surface, Raman spectra of QDs exhibit a prominent peak at 940 $cm^{-1}$ and weak broad peaks at 1352 $cm^{-1}$ and 1435 $cm^{-1}$, which could be attributed to acetate ions. These peaks correspond to ν(C–C) stretching, $\delta(CH_3)$ symmetric bending and ν(CO) symmetric stretching, respectively (35). Raman measurements support the incorporation of $Mg^{2+}$ ions in ZnO lattice and demonstrate that the QD surface is efficiently capped with OA. They also evidence the presence of acetate surface groups.

The optical properties of the ZnO and Mg-ZnO QD colloidal suspensions were studied by UV-Vis absorption and PL spectroscopy. UV-vis absorption spectra of ZnO and Mg-doped ZnO QD suspensions are shown in Figure 7. The absorption edge shifts from 340 nm to 305 nm with Mg concentration increasing from 0 to 20 mol%. This progressive blue-shift is indicative of the band gap widening upon Mg doping. The band gap energy was estimated to be the energy at which the absorbance of the absorption edge reached half of its maximum value (36). An increase from 3.37 eV to 3.71 eV is observed, consistent with previous studies (Table 1).

Usually, the PL spectra of ZnO exhibit two components. One is the exciton, or band-edge, emission in the UV range, the other is visible emission, also called deep-level emission, due to the existence of defects which are mainly located on the ZnO surface. Nanoparticles prepared by the sol-gel route exhibit mainly visible luminescence whereas their UV emission is weak. On the contrary, highly crystalline ZnO displays strong band-edge luminescence. In our study, only a weak UV emission peak at ~380 nm was observed when the ZnO QDs where excited at 342 nm. The intensity of the UV emission peak further decreased and became negligible when the concentration of Mg in QDs increased, in agreement with a previous report (37). Mg-doped QDs were excited at low wavelength, between 324 nm and 346 nm. We have therefore focused on the visible emission, by selectively exciting the defect states. Photoluminescence excitation (PLE) spectra were measured with detection at a wavelength where the visible emission was maximum (Table 1), revealing an increase in the peak energy with increasing Mg doping level (Figure 8). This dependence is in line with that of the absorption spectra.

Photoluminescence emission spectra were then collected by exciting each QD suspension at the wavelength corresponding to the maximum of the PLE spectrum (Figure 8). The emission spectra exhibit two broad bands at 400–495 nm and 495–590 nm, whose relative intensities depend on $Mg^{2+}$ concentration. The intensity of the first band is enhanced at high $Mg^{2+}$ concentration. The luminescence increases when $Mg^{2+}$ concentration rises from 5% to 20%. The quantum yields of the different samples are reported in Table 1. Remarkably, the quantum yield (QY) of 20 mol% Mg-doped ZnO colloidal suspension (64%) is about 6 times higher than that of the ZnO suspension (10%).

Figure 9 shows the emission spectra of ZnO and 20% Mg-ZnO QDs capped by OA dispersed in chloroform excited at 345 nm and 341 nm, respectively. The emission wavelength range is not affected by OA. The corresponding

**Table 2:** Raman shift ($cm^{-1}$) and assignment of the main vibrations observed in the following samples: ZnO standard, ZnO QDs, Mg-ZnO QDs, OA, OA-ZnO QDs and OA-Mg-ZnO QDs. Raman shifts are compared with values from References (32–35).

| Raman shift, $cm^{-1}$ | Origin | Reference, $cm^{-1}$ | Assignment | Reference |
|---|---|---|---|---|
| 332 | ZnO | 332 | $E_2$ (high)–$E_2$ (low) | Cusco |
| 380 | ZnO | 380 | $A_1$(TO) | Cusco |
| 410 | ZnO | 408 | $E_1$(TO) | Cusco |
| 439 | ZnO | 437 | $E_2$(high) | Cusco |
| 581 | ZnO | 584 | $E_1$(LO) | Cusco |
| 620 | Acetate | 621 | $Y_{1,5}(B_2)$; out of plane | Koleva |
| 673 | ZnO/acetate | 666/671 | TA+LO/$\upsilon_5(A_2)$; OCO sym. bend | Cusco/Koleva |
| 941 | Acetate | 942 | $\upsilon_4$ ($A_2$), C–C strech | Koleva |
| 1065 | OA | 1063 | $\upsilon_{as}$(CC), chain ordered | Tandon |
| 1085 | OA | 1082 | $\upsilon$(CC), chain ordered | Tandon |
| 1116 | OA | 1118 | $\upsilon$(CC), chain ordered | Tandon |
| 1267 | OA | 1265 | $\delta$(=CH) | De Gelder |
| 1301 | OA | 1301 | $\delta(CH_2)_n$ | De Gelder |
| 1435 | Acetate | 1435 | $\upsilon_3(A_2)$; CO sym. strech | Koleva |
| 1439 | OA | 1438 | $CH_2$ scissoring | Tandon |
| 1655 | OA | 1655 | $\upsilon$(C=C) | De Gelder |

QY values are reported in Table 3. It can be seen that OA reduced the QY of doped ZnO QDs from 64% to about 40%.

## Discussion

Doping ZnO is an effective approach to modify its properties. The introduction of dopant ions can either enlarge or narrow the band gap of the semiconductor, thereby tuning the emission colors. Furthermore, doping ZnO nanoparticles with ions such as $Mn^{2+}$, $Ni^{2+}$ or $Co^{2+}$ is known to impart magnetic properties to the material (38, 39).

Effective dopant incorporation is a critical issue. If dopant ions are excluded during ZnO crystal growth or just adsorbed on the surface, the desired properties may be compromised. The close radii of $Mg^{2+}$ (0.57 Å) and $Zn^{2+}$ (0.60 Å) contribute to the solid solubility of $Mg^{2+}$ in ZnO since $Mg^{2+}$ ions may replace $Zn^{2+}$ ions in the wurtzite lattice. However, both the ratio of actual Mg amount in nanoparticles to nominal concentration in the reaction medium and the maximum Mg doping were found extremely sensitive to the conditions of sample preparation in previous studies. Generally, higher $Mg^{2+}$ contents were achieved when the nanocrystal synthesis was performed at high temperature.

Yang et al reported a dopant content of 22.6 mol%, for a nominal 50% content in the reaction mixture. Doped nanocrystals with different shapes were obtained

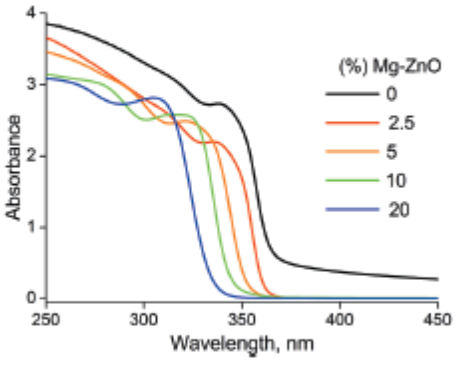


**Figure 7:** Absorption spectra of ZnO and 2.5, 5, 10 and 20% Mg-ZnO colloidal suspensions.

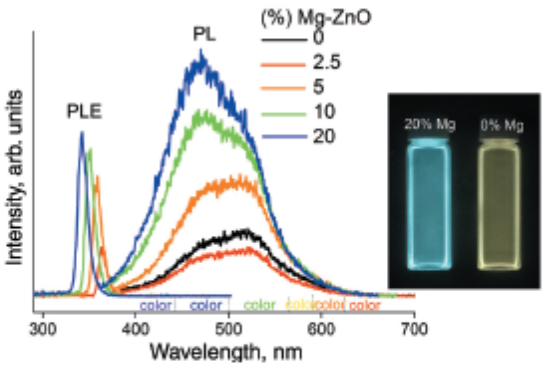


**Figure 8:** PLE and PL spectra of ZnO and 2.5, 5, 10 and 20% Mg-ZnO colloidal suspensions. The inset shows the photography of ZnO (right) and 20% Mg-ZnO (left) colloidal suspensions under UV lamp ($\lambda_{exc}$=365 nm).

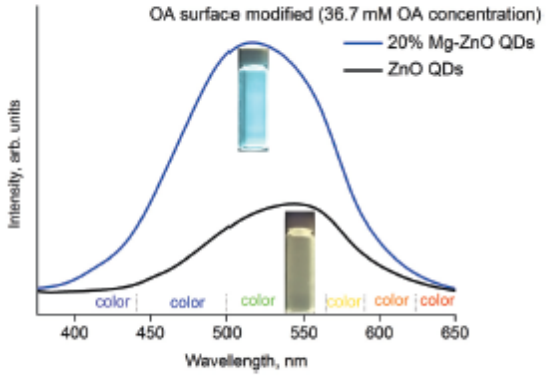


**Figure 9:** PL spectra of the OA-ZnO QDs and OA-Mg-ZnO QDs dispersed in chloroform. The insets show the photographs of each sample under UV lamp ($\lambda_{exc}$=365 nm).

by alcoholysis of Zn stearate and Mg stearate in 1-octadecene at 270°C (40). Cohn et al achieved a dopant content of 18%, close to the nominal content, by heating nanocrystals in dodecylamine at 160°C for about 20 min after hydrolysis and condensation reaction in DMSO at 50°C (41). In contrast, Mg content as low as 0.03%, for a Mg concentration in the initial solution of 20%, was obtained by Ghosh et al using sol-gel process at 70°C (42). In all cases the wurtzite ZnO phase was maintained. In the present study, the actual Mg content was always much lower than the nominal precursor concentration in the reaction medium. When synthesis was carried out with a [LiOH]/[Zn+Mg] molar ratio r=1.4, the maximum $Mg^{2+}$ substitution achieved was 2.94% for an initial Mg concentration of 20%. Synthesis performed with a different molar ratio, r=0.5, yielded a concentration of 0.56%. These findings suggested that kinetic factors, likely related to relative precursor reactivities, could limit Mg incorporation in the host ZnO crystal. Generally, it has been emphasized that the growth rate of the host crystal and the rate of deposition of dopant ions should be balanced to achieve effective doping during crystal growth (43).

**Table 3:** Quantum Yield (QY) of the ZnO and 20% Mg-ZnO QDs capped with oleic acid (OA).

| Sample | QY, % |
|---|---|
| ZnO 50 mM OA 13 mM | 5.76 |
| ZnO 50 mM OA 36.7 mM | 11.86 |
| Mg ZnO 50 mM OA 13 mM | 41.56 |
| Mg ZnO 50 mM OA 36.7 mM | 38.22 |

The presence of $Mg^{2+}$ ions affected the growth and size of the NPs, along with their structure. $Mg^{2+}$ addition decreased the final size of QDs and inhibited their fractal aggregation, suggesting a modification of their surface properties. As evidenced by X-ray diffraction, HRTEM images and Raman spectra, doped QDs displayed a less crystalline, more disordered wurtzite structure than ZnO QDs.

The incorporation of Mg widened the band gap of doped ZnO QDs primarily by decreasing their size since NPs smaller than ~6 nm are sensitive to quantum confinement. Moreover, it is known that doping with Mg widens the band gap of ZnO (37, 40). According to Cohn et al., the introduction of $Mg^{2+}$ ions raises the conduction band potential and lowers the valence band potential of ZnO (41). The two effects (quantum confinement and intrinsic effect of Mg) could not be separated.

The visible emission spanned the 400–590 nm range, featuring two broad bands at 400–495 nm and 495–590 nm whose relative intensities depended on $Mg^{2+}$ concentration. Different relaxation processes, radiative or non-radiative, can take place upon photoexcitation of a ZnO nanoparticle. Two mechanisms have been proposed for the ZnO visible emission: i) recombination of an electron in the valence band with a hole in a deep trap, ii) recombination of an electron in singly ionized oxygen vacancy (i.e., deeply trapped) with a photo-generated hole in the valence band (Xiong, 2010). The green-yellow luminescence of ZnO is usually attributed to singly ionized oxygen vacancies (15, 44–48). It has been shown by PL microscopy probing luminescence profile at single QD level that the visible emission of ZnO QDs is intrinsically broad. The broad bandwidth does not mainly arise from the NP size (or composition herein) distribution but from multiple transitions involving closely spaced energy levels, inherent to every QD, lying between the valence band and the conduction band (44). The increase in QY upon $Mg^{2+}$ doping can be explained by the increased concentration of inner and surface defects, in particular oxygen vacancies, and by the decrease in QD size. Because of the larger surface-to-volume ratio, smaller QDs entail the formation of more numerous surface defects. The surface state is expected to strongly influence the luminescence of ZnO QDs. For instance, correlations have been observed between the presence of surface hydroxide moieties and visible luminescence intensity. As observed by Felbier et al., when surface oxygen containing species, such as OH groups, were desorbed under vacuum, the visible emission vanished while the UV emission was significantly enhanced (49). Of note, the decrease in QY when Mg-doped QDs are capped by oleic acid is consistent with the hypothesis of

the role of OH groups in visible emission. The number of OH surface groups is expected to decrease if they react with oleic acid. The difference in relative intensities of the two broad bands at 400–495 nm and 495–590 nm suggests the existence of different types of defects and/or different paths for electron-hole recombination as a function of Mg concentration.

## Conclusions

Mg-ZnO QDs were synthesized by a hydrolysis and condensation reaction. $Mg^{2+}$ ions could be incorporated into the ZnO wurtzite lattice owing to the very close values of the $Mg^{2+}$ and $Zn^{2+}$ ion radii. However, the dopant ions strongly influenced the growth and final size of ZnO nanocrystals. Doping with $Mg^{2+}$ ions widened the band gap of ZnO QDs and enhanced their visible luminescence. The luminescence went through a maximum for a 20 mol% nominal concentration of $Mg^{2+}$ ions in the reaction medium. With increasing proportion of $Mg^{2+}$ ions, both the absorption and emission spectra experienced a blue shift. Mg-ZnO QDs capped by oleic acid (OA) formed stable colloidal dispersions in chloroform and toluene, with strong visible luminescence, promising for biological imaging.

## List of non-standard abbreviations

Mg-ZnO QDs, Mg-doped ZnO quantum dots; OA-ZnO QDs, ZnO quantum dots with oleic acid as surface modifier; OA-Mg-ZnO QDs, Mg-doped ZnO quantum dots with oleic acid as surface modifier.

**Acknowledgments:** The authors thank D. Desmaële for his help during synthesis, the synchrotron SOLEIL for providing beamtime at the SWING beamline (project number: 20131299) J. Perez, Y. Liatimi and P. Roblin for their support during SAXS experiments, S. Blanchandin for WAXS measurements, the Service of electronic microscopy of the University Pierre et Marie Curie for HRTEM measurements, and FAPESP and PADC/FCF-UNESP for the financial support. This work was conducted during a scholarship of E. Berbel Manaia supported by the International Cooperation Program CAPES/COFECUB (ME 767-13) at the University Paris – Sud, financed by CAPES – Brazilian Federal Agency for Support and Evaluation of Graduate Education within the Ministry of Education of Brazil.

## References

1. Reid PJ, Fujimoto B, Gamelin DR. A simple ZnO nanocrystal synthesis illustrating three-dimensional quantum confinement. J Chem Educ 2013;91:280–2.
2. Michalet X, Pinaud FF, Bentolila LA, Tsay JM, Doose S, Li JJ, et al. Quantum dots for live cells, in vivo imaging, and diagnostics. Science 2005;307:538–44.
3. Wang C, Gao X, Su X. In vitro and in vivo imaging with quantum dots. Anal Bioanal Chem 2010;397:1397–415.
4. Xie J, Lee S, Chen X. Nanoparticle-based theranostic agents. Adv Drug Deliv Rev 2010;62:1064–79.
5. Tian B, Al-Jamal WT, Al-Jamal KT, Kostarelos K. Doxorubicin-loaded lipid-quantum dot hybrids: surface topography and release properties. Int J Pharm 2011;416:443–7.
6. Park JH, von|Maltzahn G, Ruoslahti E, Bhatia SN, Sailor MJ. Micellar hybrid nanoparticles for simultaneous magnetofluorescent imaging and drug delivery. Angew Chem Int Ed 2008;47:7284–8.
7. Bagalkot V, Zhang L, Levy-Nissenbaum E, Jon S, Kantoff PW, Langer R, et al. Quantum dot-aptamer conjugates for synchronous cancer imaging, therapy, and sensing of drug delivery based on bi-fluorescence resonance energy transfer. Nano Lett 2007;7:3065–70.
8. Su Y, He Y, Lu H, Sai L, Li Q, Li W, et al. The cytotoxicity of cadmium based, aqueous phase – synthesized, quantum dots and its modulation by surface coating. Biomaterials 2009;30:19–25.
9. Chang E, Thekkek N, Yu WW, Colvin VL, Drezek R. Evaluation of quantum dot cytotoxicity based on intracellular uptake. Small 2006;2:1412–7.
10. Lewinski N, Colvin V, Drezek R. Cytotoxicity of nanoparticles. Small 2008;4:26–49.
11. Klaine SJ, Alvarez PJ, Batley GE, Fernandes TF, Handy RD, Lyon DY, et al. Nanomaterials in the environment: behavior, fate, bioavailability, and effects. Environ Toxicol Chem 2008;27:1825–51.
12. Jia Z, Misra RD. Tunable ZnO quantum dots for bioimaging: synthesis and photoluminescence. Mater Tech 2013;28:221–7.
13. Xiong HM. ZnO nanoparticles applied to bioimaging and drug delivery. Adv Mater 2013;25:5329–35.
14. Moussodia RO, Balan L, Merlin C, Mustin C, Schneider R. Biocompatible and stable ZnO quantum dots generated by functionalization with siloxane-core PAMAM dendrons. J Mater Chem 2010;20:1147–55.
15. Zhang L, Yin L, Wang C, lun N, Qi Y, Xiang D. Origin of visible photoluminescence of ZnO quantum dots: defect-dependent and size-dependent. J Phys Chem C 2010;114:9651–8.
16. Caetano BL, Santilli CV, Meneau F, Briois VR, Pulcinelli SH. In Situ and Simultaneous UV-vis/SAXS and UV-vis/XAFS time-resolved monitoring of ZnO quantum dots formation and growth. J Phys Chem C 2011;115:4404–12.
17. Xiong HM. Photoluminescent ZnO nanoparticles modified by polymers. J Mater Chem 2010;20:4251–62.
18. Vijayalakshmi K, Karthick K. Influence of Mg doping on the microstructure and PL emission of wurtzite ZnO synthesized by microwave processing. J Mater Sci Mater Electron 2013;24:2067–71.
19. Xiong HM, Shchukin DG, Möhwald H, Xu Y, Xia YY. Sonochemical synthesis of highly luminescent zinc oxide nanoparticles doped with magnesium(II). Angew Chem 2009;121:2765–9.

20. Lin YJ, Wu PH, Tsai CL, Liu CJ, Lin ZR, Chang HC, et al. Effects of Mg incorporation on the optical properties of ZnO prepared by the sol-gel method. J Appl Phys 2008;103:113709.
21. Ding R, Xu C, Gu B, Shi Z, Wang H, Ba L, et al. Effects of Mg incorporation on microstructure and optical properties of ZnO thin films prepared by sol-gel method. J Mater Sci Technol 2010;26:601–4.
22. Yousefi R, Jamali Sheini F, Muhamad MR, More MA. Characterization and field emission properties of ZnMgO nanowires fabricated by thermal evaporation process. Solid State Sci 2010;12:1088–93.
23. Spanhel L, Anderson MA. Semiconductor clusters in the sol-gel process: quantized aggregation, gelation, and crystal growth in concentrated zinc oxide colloids. J Am Chem Soc 1991;113:2826–33.
24. Meulenkamp EA. Synthesis and growth of Zno nanoparticles. J Phys Chem B 1998;102:5566–72.
25. Kohlbrecher J, Bressler I. SASfit. Paul scherrer institut, Villigen: Switzerland. 2014.
26. Sun LW, Shi HQ, Li WN, Xiao HM, Fu SY, Caoc XZ, et al. Lanthanum-doped ZnO quantum dots with greatly enhanced fluorescent quantum yield. J Mater Chem 2012;22:8221–7.
27. Crosby GA, Demas JN. Measurement of photoluminescence quantum yields. Rev J Phys Chem 1971;75:991–1024.
28. West AR. Solid state chemistry and its applications. New York: John Wiley and Sons, 1992.
29. Guinier A, Fournet G. Small angle scattering of X-rays. New York: Wiley, 1955.
30. Craievich AF. In: Handbook of sol-gel science and technology. Sakka A, Almeida R, editors. Norwell, MA: Kluwer Publishers, 2005.
31. Brinker CJ, Scherer GW. Sol-gel sciences. The physics and chemistry of sol-gel processing. San Diego: Academic Press, Inc., 1990.
32. Cuscó R, Alarcón-Lladó E, Ibáñez J, Artús L. Temperature dependence of Raman scattering in ZnO. Phys Rev B 2007;75:165202.
33. De Gelder J, De Gussem K, Vandenabeele P, Moens L. Reference database of Raman spectra of biological molecules. J Raman Spectrosc 2007;38:1133–47.
34. Tandon P, Förster G, Neubert R, Wartewig S. Phase transitions in oleic acid as studied by X-ray diffraction and FT-Raman spectroscopy. J Mol Struct 2000;524:201–15.
35. Koleva V, Stoilova D. Infrared and Raman studies of the solids in the Mg(CH3COO)2-Zn(CH3COO)2-H2O system. J Mol Struct. 2002;611:1–8.
36. Brus L. Electronic wave functions in semiconductor clusters: experiment and theory. J Phys Chem 1986;90:2555–60.
37. Yousefi R, Zak AK, Jamali-Sheini F. Growth, X-ray peak broadening studies, and optical properties of Mg-doped ZnO nanoparticles. Mater Sci Semicond Process 2013;16:771–7.
38. Schwartz DA, Norberg NS, Nguyen QP, Parker JM, Gamelin DR. Magnetic quantum dots: synthesis, spectroscopy, and magnetism of $Co^{2+}$- and $Ni^{2+}$-doped ZnO nanocrystals. J Am Chem Soc 2003;125:13205–18.
39. Norberg NS, Kittilstved KR, Amonette JE, Kukkadapu RK, Schwartz DA, Gamelin DR. Synthesis of colloidal $Mn^{2+}$:ZnO quantum dots and high-TC ferromagnetic nanocrystalline thin films. J Am Chem Soc 2004;126:9387–98.
40. Yang Y, Jin Y, He H, Wang Q, Tu Y, Lu H, et al. Dopant-induced shape evolution of colloidal nanocrystals: the case of zinc oxide. J Am Chem Soc 2010;132:13381–94.
41. Cohn AW, Kittilstved KR, Gamelin DR. Tuning the potentials of "Extra" electrons in colloidal n-Type ZnO nanocrystals via $Mg^{2+}$ substitution. J Am Chem Soc 2012;134:7937–43.
42. Ghosh M, Raychaudhuri AK. Optical properties of Mg-substituted ZnO nanoparticles obtained by solution growth. Nanotech IEEE Trans Nanotechnol 2011;10:555–9.
43. Buonsanti R, Milliron DJ. Chemistry of doped colloidal nanocrystals. Chem Mater 2013;25:1305–17.
44. Layek A, De S, Thorat R, Chowdhury A. Spectrally resolved photoluminescence imaging of ZnO nanocrystals at single-particle levels. J Phys Chem Lett 2011;2:1241–7.
45. van Dijken A, Meulenkamp EA, Vanmaekelbergh D, Meijerink A. The kinetics of the radiative and non-radiative processes in nanocrystalline ZnO particles upon photoexcitation. J Phys Chem B 2000;104:1715–23.
46. Xu X, Xu C, Wang X, Lin Y, Dai J, Hu J. Control mechanism behind broad fluorescence from violet to orange in ZnO quantum dots. Cryst Eng Comm 2013;15:977–81.
47. Liu DP, Li GD, Su Y, Chen JS. Highly luminescent ZnO nanocrystals stabilized by ionic-liquid components. Angew Chem Int Ed 2006;45:7370–3.
48. Yousefi R, Kamaluddin B. Fabrication and characterization of ZnO and ZnMgO nanostructures grown using a ZnO/ZnMgO compound as the source material. Appl Surf Sci 2009;256:329–34.
49. Felbier P, Yang J, Theis J, Liptak W, Wagne A, Lorke A, et al. Highly Luminescent ZnO quantum dots made in a non-thermal plasma. Adv Funct Mater 2014;24:1988–93.

## Bionotes

**Eloísa Berbel Manaia**
Faculty of Pharmaceutical Sciences of São Paulo State University, UNESP, Araraquara-Jaú Interstate Highway, Km 1, Araraquara, SP, Brazil
University Paris-Sud, Institut Galien, CNRS, UMR 8612, LabEX LERMIT, F-92296 Châtenay-Malabry, France

Eloísa Berbel Manaia is currently preparing her PhD thesis in co-direction between the Faculty of Pharmaceutical Sciences, São Paulo State University (Brazil) and the Faculty of Pharmacy, Institut Galien, University Paris Sud (France). The topic of her PhD thesis and her research interest focus on the development of QDs based on ZnO for application in bioimaging and also in theranostic systems using lipid nanocarriers. She is particularly interested in nanomedicine, diagnostic molecules and drug delivery systems.

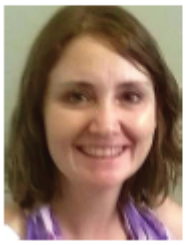

**Renata Cristina Kiatkoski Kaminski**
Sergipe Federal University, Campus Itabaiana, Av. Vereador Olimpio Grande, s/n, Itabaiana, SE, Brazil

Renata C.K. Kaminski received a Chemistry diploma from the University of Paraná (UFPR) in 2000. She completed her PhD degree in Chemistry at the São Paulo State University (2006) studying $TiO_2$-based thin films and powder. In 2008 she had a post-doctoral position at the Synchrotron SOLEIL (Saint-Aubin), where she worked as chemical engineer and researcher for 1 year. Now, she works as researcher at University of Sergipe (UFS), her research foccuses on $TiO_2$-based nanoparticles for photoprotection and antioxidants delivery via emulsified or liquid crystalline systems.

**Bruno Leonardo Caetano**
Chemistry Institute of São Paulo State University, UNESP, Prof. Francisco Degni Street, 55, Araraquara, SP, Brazil

Bruno Leonardo Caetano received a Chemistry diploma from the University of Franca (2003). He completed his PhD degree in Chemistry at the São Paulo State University (2010) studying the formation and growth of ZnO quantum dots. He completed his first post-doctoral in 2011 at the Synchrotron SOLEIL (Saint-Aubin). Now, his research for his second post-doctorate is focused on the nucleation and growth of nanoparticles, organic-inorganic hybrid materials and magnetic nanoparticles for drug delivery systems and hyperthermia.

**Valérie Briois**
Synchrotron SOLEIL, L'Orme des Merisiers, BP48, Saint Aubin, 91192 Gif-sur Yvette, France

Valérie Briois received a Chemical Engineering diploma from the National School of Chemistry of Paris (ENSCP) in 1988. She completed her PhD degree in Chemistry at the Université Pierre et Marie Curie-Paris VI in 1991 on the study of the genesis of oxysulfate of cerium(IV) by synchrotron radiation techniques. Then she joined the CNRS as researcher first at the Laboratoire pour l'Utilisation du Rayonnement Electromagnétique (LURE, Orsay) and then at the Synchrotron SOLEIL (Saint-Aubin) where she took the responsibility of hard X-rays beamlines dedicated to the X-ray absorption spectroscopy (XAS). She focuses her research interests on nanostructured materials prepared by soft-chemistry routes aiming to establish relationships between local range order structures determined by XAS and nanomaterials properties.

**Leila Aparecida Chiavacci**
Faculty of Pharmaceutical Sciences of São Paulo State University, UNESP, Araraquara-Jaú Interstate Highway, Km 1, Araraquara, SP, Brazil

Leila Aparecida Chiavacci graduated in Chemistry at São Paulo State University (UNESP) (1993), obtained her MSc in Chemistry/Physical Chemistry at UNESP (1996), and she completed her PhD in Chemistry/Physical Chemistry and in Materials Science in co-direction between UNESP and LURE, Université Paris-Sud (2001). Currently, she is a Professor at the Faculty of Pharmaceutical Sciences – UNESP – Araraquara. She has experience in the area of Chemistry and Materials, with an emphasis in Physical Chemistry and Nanomaterials, acting on the following topics: colloids, nanomaterials, controlled release of drugs, SAXS, EXAFS, and sol-gel hybrid organic-inorganic materials.

**Claudie Bourgaux**
University Paris-Sud, Institut Galien, CNRS, UMR 8612, LabEX LERMIT, F-92296 Châtenay-Malabry, France,
**claudie.bourgaux@u-psud.fr**

Claudie Bourgaux joined the CNRS as researcher in 1982, first at ESPCI (PARIS) and then at the "Laboratoire pour l'Utilisation du Rayonnement Electromagnétique" (LURE, ORSAY) as co-responsible of SAXS beamline. Currently, she works at "Institut Galien Paris-Sud". Her research interests include supramolecular assemblies of lipids and amphiphiles, either for the delivery and controlled release of drugs or for the study of interactions of drugs with model membranes.

ÉCOLE DOCTORALE
Sciences chimiques : molécules, matériaux, instrumentation et biosystèmes

**Titre :**Conception de Quantum dots à base d'oxyde de zinc (ZnO) pour des applications en bio-imagerie de nanosystèmes lipidiques

**Mots clés :**ZnO, Quantum Dots, bioimagerie et nanosystèmes lipidiques

**Résumé :**Les systèmes théranostiques, consistant en un dispositif unique contenant des agents de diagnostic et des principes actifs, suscitent un interêt accru car ils peuvent améliorer le traitement de maladies telles que le cancer. L'objectif de ce travail était d'insérer des Quantum Dots (QDs) à base de ZnO dans des nanoparticules lipidiques pouvant délivrer un principe actif anti-cancéreux. Nous avons étudié des QDs présentant une structure coeur-coquille ZnO/ZnS, des QDs dopés par des ions Mg, la modification de leur surface par de l'acide oléique (OA) et leur incorporation dans des nanoparticules lipidiques pour suivre l'internalisation des nanoparticules par les macrophages.

**Title :**Zinc oxide (ZnO) based quantum dots for bioimaging applications of lipid nanocarriers

**Keywords :**ZnO, Quantum Dots, bioimaing, and lipid nanocarriers

**Abstract :**Theranostic systems consist of a single device containing therapeutic and diagnosis agents and receive increased attention because these devices can improve the therapy of diseases such as cancer. The aim of this work was to incorporateZnO based quantum dots (QDs) into lipid based nanocarriersallowing to encapsulate a model drug for cancer therapy. It was studied QDs presenting ZnO/ZnS core-shell structure, Mg-doped ZnO QDs, oleic acid (OA) surface modified QDs and their incorporation into lipid nanoparticles to study the internalization of the luminescent nanoparticles by macrophages.

**Université Paris-Saclay**
Institut Galien Paris Sud, UMR CNRS 8612
5, Rue Jean Baptiste Clément / 92296 Châtenay-Malabry, France